

Custodial Naturalness

The de Boer,^a Manfred Lindner^a and Andreas Trautner^{a,b}

^a*Max-Planck-Institut für Kernphysik, Saupfercheckweg 1, 69117 Heidelberg, Germany*

^b*CFTP, Departamento de Física, Instituto Superior Técnico, Universidade de Lisboa, Avenida Rovisco Pais 1, 1049 Lisboa, Portugal*

E-mail: thede.deboer@mpi-hd.mpg.de, lindner@mpi-hd.mpg.de,
trautner@mpi-hd.mpg.de

ABSTRACT: Custodial Naturalness is a new symmetry-based idea to explain the large separation between the electroweak (EW) scale and ultraviolet completions of the Standard Model (SM). Classical scale invariance is combined with an enhanced scalar-sector custodial symmetry and both are spontaneously broken by dimensional transmutation at a new intermediate scale. The SM-like Higgs boson is an elementary pseudo-Nambu-Goldstone-Boson (pNGB) of the extended custodial symmetry, which naturally explains the suppression of the EW scale without a little hierarchy problem. We explain details of the general mechanism, its minimal realization and simplest extensions which populate Higgs-, gauge-, and neutrino portals and introduce candidates for particle Dark Matter (DM). We show the stability of the mechanism under inclusion of new sources of explicit custodial symmetry violation, as well as under variations of boundary conditions at the high scale. Custodial Naturalness is experimentally testable – including a specific correlation between the Higgs and top quark masses, as well as by the prediction of a new heavy Z' gauge boson and a new dilaton-like scalar which are well-motivated targets for future colliders and Higgs factories. The cosmological evolution features a strongly supercooled phase transition implying that consequences of Custodial Naturalness may also be tested by gravitational wave observatories.

Contents

1	Introduction	1
2	General discussion	3
2.1	Non-conformal case	3
2.2	Scalar sector and symmetry breaking	4
2.3	Charge assignment	5
2.4	Different sources of custodial symmetry violation	7
2.4.1	SM sector	7
2.4.2	New gauge sector	7
2.4.3	New Yukawa interactions	8
2.5	The effective potential	9
2.6	Masses and mixing	11
2.6.1	Scalar masses	12
2.6.2	Vector masses	12
3	Different models realizing Custodial Naturalness	13
3.1	Minimal model	13
3.2	Minimal fermion extension - Neutrino portal model	15
3.3	Dark matter model	16
4	New particle masses and further experimental signatures	20
5	Cosmological evolution and gravitational wave signatures	24
6	Variations and embeddings of Custodial Naturalness	25
7	Conclusions	26

1 Introduction

Remarkably, the Standard Model (SM) exhibits scale invariance at the classical level, explicitly broken only by the Higgs mass term as well as by quantum corrections. The Higgs mass does not receive quadratically divergent corrections if there are no additional terms that break scale invariance [1]. Additional scales larger than the electroweak (EW) scale lead to corrections to the Higgs mass, giving rise to the hierarchy problem.

The anomalous breaking of classical scale invariance¹ can be translated to a physical scale via dimensional transmutation. As shown by Coleman and Weinberg [2], in the weak

¹In this work, we use the term “conformal symmetry” and classical scale invariance interchangeably.

coupling regime, a massless scalar field can obtain a vacuum expectation value (VEV), if the beta function of the scalar quartic coupling is dominated by bosonic contributions. In the SM, the top Yukawa coupling dominates the running of the Higgs quartic coupling and thus the minimal realization, i.e. the SM without the Higgs mass term, is excluded [3, 4]. In models with additional scalar fields, dimensional transmutation in the new sector can generate an intermediate scale and the portal coupling then induces the Higgs mass (see, for example, Refs. [5–15]). Quantum corrections involving new fields with masses of the intermediate scale contribute to the Higgs mass giving rise to the little hierarchy problem. These contributions scale as $\sim \frac{1}{16\pi^2} g^2 m_\psi^2$ where m_ψ is the mass of the heavy field and g is the coupling of the heavy field to the Higgs field.

A popular approach to the little hierarchy problem is based on spontaneously broken approximate symmetries. The Higgs boson is then a pseudo-Nambu-Goldstone-Boson (pNGB) with a mass naturally smaller than the scale of new physics. Popular examples are strong coupling solutions such as composite Higgs [16–19] and little Higgs [20–22] as well as twin Higgs models [23–25]. These solutions typically require a top partner in the TeV mass range.

Recently, we proposed Custodial Naturalness [26] as a mechanism to explain both the separation of the EW and Planck scale as well as the little hierarchy problem. The simple setup of models with scale invariance and an elementary Higgs boson is combined with the idea of the Higgs boson as a pNGB of a spontaneously broken global symmetry. The top Yukawa coupling is marginal, similar to the SM, and can very well be present in the ultraviolet (UV) theory. While it violates the enhanced global symmetry explicitly, it does not necessarily lead to a large correction to the Higgs mass for the same reasons as discussed by Bardeen [1]. Previous works have considered an elementary Higgs boson as a pNGB [27, 28] compared to which we include scale invariance and dimensional transmutation, use a simpler scalar sector and impose an extended custodial symmetry at the high scale. Particle content and fermion charge assignment in the simplest realization of Custodial Naturalness closely resemble the “minimal $B - L$ model” [29–35] and its conformal realization [11, 12], while the details of the scalar sector differ.

In this work we extend the results of Ref. [26], highlighting different aspects of custodial symmetry violation and their impact on the little hierarchy. We extend the original minimal model to incorporate new sources of custodial symmetry violation opening the possibility for the new sector to populate the neutrino mass matrix or allow for Dark Matter (DM). In total, we discuss three models - the minimal model, the neutrino portal model and the DM model.

After symmetry breaking, the particle content includes the SM in addition to a new gauge boson Z' in the $\sim 4 - 100$ TeV range as well as the dilaton with a mass that is loop suppressed compared to the Z' mass and typically in the $\sim 30 - 1000$ GeV range. The neutrino portal extension of the minimal model introduces heavy and massless new fermions while the DM model introduces a fermionic two-component DM candidate.

This work is structured as follows: Section 2 presents the concept of Custodial Naturalness including an analytical discussion of the effective potential. Special emphasis is placed on the different sources of custodial symmetry violation. In Sec. 3 we introduce

different models that realize our idea. The effect of custodial symmetry violation is studied numerically and the amount of fine tuning is quantified. In Sec. 4 we give numerical results for the masses of new particles and discuss experimental signatures of our model. Section 5 sketches the thermal history of the Universe, and in Sec. 6 we discuss variations of the general idea and embeddings. In Sec. 7 we draw our conclusions.

2 General discussion

The concept of Custodial Naturalness combines conformal and custodial symmetry in an enlarged scalar sector consisting of the SM Higgs doublet H and an additional complex scalar singlet Φ . The field Φ obtains a VEV spontaneously breaking custodial symmetry and the Higgs field is a pNGB associated with this breaking. Before studying the scale invariant case, we briefly discuss the scalar potential with tree level mass terms. This allows us to understand how the mass of the Higgs field is protected by custodial symmetry.

2.1 Non-conformal case

The general tree level potential is given by

$$V = -m_H^2 |H|^2 - m_\Phi^2 |\Phi|^2 + \lambda_H |H|^4 + 2\lambda_p |H|^2 |\Phi|^2 + \lambda_\Phi |\Phi|^4. \quad (2.1)$$

Given that $m_\Phi^2 > 0$ and $-m_H^2 + m_\Phi^2 \frac{\lambda_p}{\lambda_\Phi} > 0$, the minimum of the potential at tree level is given by $\langle \Phi \rangle := \frac{v_\Phi}{\sqrt{2}} = \sqrt{\frac{m_\Phi^2}{2\lambda_\Phi}}$, $\langle H \rangle = 0$. We now integrate out the field corresponding to excitation in the Φ direction at tree level. This gives the potential in the effective field theory for H given by

$$\begin{aligned} V_{\text{EFT}} &= (-m_H^2 + \lambda_p v_\Phi^2) |H|^2 + \left(\lambda_H + \frac{\lambda_p^2}{\lambda_\Phi} \right) |H|^4 \\ &= \left(-m_H^2 + \lambda_p \frac{m_\Phi^2}{\lambda_\Phi} \right) |H|^2 + \left(\lambda_H + \frac{\lambda_p^2}{\lambda_\Phi} \right) |H|^4. \end{aligned} \quad (2.2)$$

At tree level, the mass of H vanishes for $m_H^2 = m_\Phi^2$ and $\lambda_p = \lambda_\Phi$. Note how this is independent of the value of the coupling λ_H . If we now consider a potential that obeys an approximate symmetry of rotations between H and Φ , where only the quartic coupling for H breaks this symmetry, i.e.

$$V = -m^2 (|H|^2 + |\Phi|^2) + \lambda (|H|^2 + |\Phi|^2)^2 + (\lambda_H - \lambda) |H|^4, \quad (2.3)$$

then H remains massless at tree level. We have checked that $\langle \Phi \rangle = \sqrt{\frac{m^2}{2\lambda}}$, $\langle H \rangle = 0$ remains the minimum at tree level given that $\lambda_H > \lambda$. Generally speaking, symmetry violating interactions that only couple to the Higgs field (and not to Φ) contribute to the Higgs mass only at subleading level.

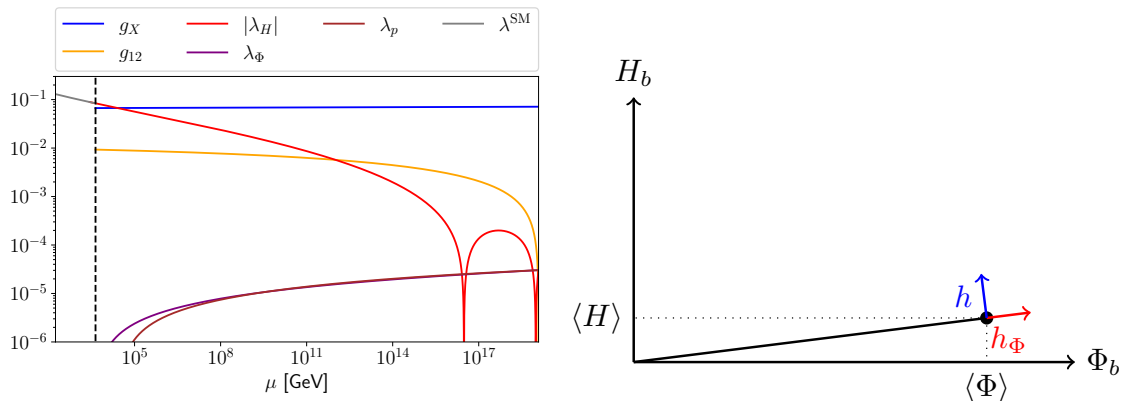


Figure 1. Left: Running of couplings for a typical model. At Planck scale, the scalar potential has a $SO(6)$ custodial symmetry $\lambda_H = \lambda_p = \lambda_\Phi$. The dashed vertical line indicates the scale of Coleman-Weinberg symmetry breaking. Right: The orientation of the VEV in the $\Phi - H$ plane and the radial excitation corresponding to the dilaton h_Φ as well as the orthogonal excitation corresponding to the pNGB Higgs boson h .

2.2 Scalar sector and symmetry breaking

Custodial Naturalness is based on the assumption that at some high scale, which we choose to be the Planck scale M_{Pl} , the potential is scale invariant and has a $SO(6)$ custodial symmetry,² explicitly

$$V = \lambda (|H|^2 + |\Phi|^2)^2 \quad \text{at} \quad \mu = M_{\text{Pl}}. \quad (2.4)$$

Classical scale invariance, which forbids the tree level mass terms, is broken by the scale anomaly, i.e. the non-vanishing beta functions. Custodial symmetry breaking is mediated to the potential by quantum corrections as manifest in the RG running (see Fig. 1) demanding a more general form of the tree level quartic potential,

$$V_{\text{tree}} = \lambda_H |H|^4 + 2\lambda_p |H|^2 |\Phi|^2 + \lambda_\Phi |\Phi|^4. \quad (2.5)$$

Nonetheless, λ_Φ and λ_p remain close to each other as the difference $\lambda_p - \lambda_\Phi$ is protected by custodial symmetry. At some intermediate scale of $\sim 10^5$ GeV, λ_p turns negative and λ_Φ turns small. At this scale the one loop potential needs to be considered in order to obtain the vacuum configuration [2].

To study the structure of the VEVs, we first use the Gildener-Weinberg approximation [4]. Adopting the typical notation, we write the scale invariant potential as

$$V = f_{ijkl} \Phi_i \Phi_j \Phi_k \Phi_l, \quad (2.6)$$

where Φ_i denotes the scalar fields³ and f_{ijkl} are the corresponding quartic couplings. At some RG scale μ_{GW} the potential develops a flat direction. We write the fields in terms of

²We refer to this symmetry as custodial symmetry because it is a symmetry of the scalar potential that is explicitly broken by the gauge and Yukawa interactions [36]. Under $SO(6)$, the six scalar degrees of freedom transform as a real **6**-plet.

³ Φ_i takes values of all scalar fields and should not be confused with the scalar singlet Φ .

the radial distance from the origin ϕ and a unit vector n_i by $\Phi_i = n_i\phi$. The condition for the flat direction is then given by

$$\left. \frac{\partial V}{\partial \Phi_j} \right|_{\Phi_i = n_i\phi} = 0 \quad \text{and} \quad V|_{\Phi_i = n_i\phi} = 0 \quad \text{at } \mu = \mu_{\text{GW}} \quad (2.7)$$

for a non zero value of ϕ . For negative λ_p , the solution to these equations is given by [37]

$$H = \sqrt{\frac{-\lambda_p}{\lambda_H - \lambda_p}}\phi, \quad \Phi = \sqrt{\frac{\lambda_H}{\lambda_H - \lambda_p}}\phi, \quad \lambda_\Phi = \frac{\lambda_p^2}{\lambda_H}. \quad (2.8)$$

Since λ_p turns out to be small, the flat direction is mostly aligned in the Φ -direction (see Fig. 1). Along this flat direction, quantum corrections generate a non-trivial minimum leading to a VEV that spontaneously breaks conformal and custodial symmetry. Custodial symmetry is broken like $\text{SO}(6) \rightarrow \text{SO}(5)$ which yields five Goldstone bosons, four of which are eaten by the longitudinal degrees of freedom of the massive gauge bosons. The final Goldstone boson is a pNGB that closely resembles the physical Higgs boson, whose mass is proportional to the size of custodial symmetry violation. The remaining massive scalar is the pNGB corresponding to the spontaneous breakdown of scale invariance. The mass of this dilaton, the radial excitation, is generated at one loop and therefore suppressed with respect to the VEV by the beta function.

2.3 Charge assignment

The particle content of our model consists of the SM fields in addition to three right-handed neutrinos ν_R and the complex scalar singlet Φ . We further add a $\text{U}(1)$ gauge group whose contributions to the RGE drive λ_Φ to its critical value ensuring symmetry breaking à la Coleman-Weinberg. For minimal models, gauge anomaly freedom requires that the SM fermions have a $\text{U}(1)$ charge which is a linear combination of $B - L$ and hypercharge. We give the $B - L$ charges of the SM fields and Φ in Tab. 1. Additional fermions are vector-like and do not contribute to the gauge anomalies. It turns out to be convenient to work in a basis where the $\text{U}(1)$ charges of the scalar fields are symmetric. In this basis, the charges under the new $\text{U}(1)_X$ group are the following linear combination

$$Q^{(X)} = 2Q^{(Y)} + \frac{1}{q_\Phi}Q^{(B-L)}, \quad (2.9)$$

where $Q^{(Y)}$ and $Q^{(B-L)}$ are the hyper- and $B - L$ charges of a generic field, while q_Φ is the $B - L$ charge of Φ which is a free parameter of the charge assignment.

In this work, we discuss three different models. The minimal realization of Custodial Naturalness simply consists of the SM fields in addition to the scalar field Φ . Further, we consider a model where we add an additional set of fermions, see Tab. 1 (middle). The $\text{U}(1)$ charges of these new fermions are chosen in such a way that ψ_L couples to right-handed neutrinos via the Yukawa interaction

$$\mathcal{L}_{\text{Yuk}} \supset y_{\psi}^{\alpha} \bar{\psi}_L \Phi^{\dagger} \nu_R^{\alpha} + \text{h.c.} \quad (2.10)$$

Table 1. Charges of SM and new fields under the new $U(1)_X$ gauge group. $B - L$ charges are linear combinations of X and Y charges and are shown as well. The “Minimal particle content” is sufficient to realize the idea of Custodial Naturalness. Also shown are minimal extensions that allow for new neutrino Yukawa couplings or an explanation of DM. Here, q_Φ and p are free parameters of the charge assignment (see text for details).

Name	Generations	$SU(3)_c \times SU(2)_L \times U(1)_Y \times U(1)_X$	$U(1)_{B-L}$
Minimal particle content			
Q	3	$(\mathbf{3}, \mathbf{2}, +\frac{1}{6})$	$+\frac{1}{3} + \frac{1}{3q_\Phi}$
L	3	$(\mathbf{1}, \mathbf{2}, -\frac{1}{2})$	$-1 - \frac{1}{q_\Phi}$
u_R	3	$(\mathbf{3}, \mathbf{1}, +\frac{2}{3})$	$+\frac{4}{3} + \frac{1}{3q_\Phi}$
d_R	3	$(\mathbf{3}, \mathbf{1}, -\frac{1}{3})$	$-\frac{2}{3} + \frac{1}{3q_\Phi}$
e_R	3	$(\mathbf{1}, \mathbf{1}, -1)$	$-2 - \frac{1}{q_\Phi}$
ν_R	3	$(\mathbf{1}, \mathbf{1}, 0)$	$-\frac{1}{q_\Phi}$
H	1	$(\mathbf{1}, \mathbf{2}, +\frac{1}{2})$	+1
Φ	1	$(\mathbf{1}, \mathbf{1}, 0)$	+1
Minimal set of additional fermions			
ψ_L	1	$(\mathbf{1}, \mathbf{1}, 0)$	$-\left(\frac{1}{q_\Phi} + 1\right)$
ψ_R	1	$(\mathbf{1}, \mathbf{1}, 0)$	$-\left(\frac{1}{q_\Phi} + 1\right)$
Additional fermions that allow for DM			
ψ_L	1	$(\mathbf{1}, \mathbf{1}, 0)$	$\frac{p}{q_\Phi}$
ψ_R	1	$(\mathbf{1}, \mathbf{1}, 0)$	$\frac{p}{q_\Phi} + 1$
ψ'_L	1	$(\mathbf{1}, \mathbf{1}, 0)$	$\frac{p}{q_\Phi} + 1$
ψ'_R	1	$(\mathbf{1}, \mathbf{1}, 0)$	$\frac{p}{q_\Phi}$

where $\alpha = 1, 2, 3$ runs over the number of generations. This model is the minimal model that allows for a Yukawa interaction involving Φ . The third model we discuss introduces two sets of new fermions (see Tab. 1 (bottom)). Here, p is a free parameter. If p is set to a value that prohibits a Yukawa coupling involving new fermions and right-handed neutrinos, then the new fermions are stable, making them natural DM candidates. In this case we have the following new Yukawa interactions

$$\mathcal{L}_{\text{Yuk}} \supset y_\psi \bar{\psi}_L \Phi^\dagger \psi_R + y_{\psi'} \bar{\psi}'_L \Phi \psi'_R + \text{h.c.} \quad (2.11)$$

2.4 Different sources of custodial symmetry violation

The $SO(6)$ custodial symmetry is explicitly violated by the gauge and Yukawa interactions present in our model. In Sec. 2.5, we will show that small values of the splitting $\lambda_\Phi - \lambda_p$ lead to a large hierarchy between the VEV of Φ and the Higgs mass. In contrast, λ_H runs to large values driven by the top Yukawa coupling and only has a subleading effect on the hierarchy. This agrees with the result for the non-conformal case (Sec. 2.1) and might already be guessed from Eq. (2.8) in the conformal case. In order for the Higgs field to obtain a VEV, $\lambda_p < \lambda_\Phi$ at the intermediate scale is required (see Eq. (2.8) and Sec. 2.5). We now discuss the different possible sources of custodial symmetry violation and how these contributions drive λ_Φ and λ_p apart.

2.4.1 SM sector

The SM fermions and (electroweak) gauge bosons only couple to the Higgs field and have no coupling to Φ . While these couplings strongly impact the running of λ_H , the effect on the running of λ_p and λ_Φ is suppressed by λ_p . The difference in the beta functions of λ_p and λ_Φ induced by SM couplings is given by

$$\beta_{\lambda_p} - \beta_{\lambda_\Phi} \Big|_{\text{SM}} \simeq \frac{1}{16\pi^2} \lambda_p \left[-\frac{9}{2} g_L^2 - \frac{3}{2} g_Y^2 + 12\lambda_H + 6y_t^2 \right], \quad (2.12)$$

where g_Y and g_L are the hypercharge and $SU(2)_L$ gauge couplings and y_t is the top Yukawa coupling. This tends to be a relatively small effect as for typical models $\lambda_p \lesssim 10^{-4}$. Such small values of λ_p are required as, in order for λ_Φ to reach its critical value at μ_{GW} , the symmetric scalar coupling at the high scale needs to fulfill $\lambda \approx \frac{6g_X^4}{16\pi^2} \ln\left(\frac{M_{\text{Pl}}}{\mu_{\text{GW}}}\right)$. For $g_X \approx 0.1$ this requires $\lambda \approx 10^{-4}$. The SM contributions to $\beta_{\lambda_p} - \beta_{\lambda_\Phi}$ are negative for $10^{11} \text{ GeV} \lesssim \mu < M_{\text{Pl}}$ and the integrated effect leads to $\lambda_p > \lambda_\Phi$. If this were the only source of custodial symmetry violation, the mass parameter for the Higgs doublet would be positive and thus there would be no EWSB. Consequently there need to be additional sources of custodial symmetry violation with opposite sign.⁴

2.4.2 New gauge sector

Another source of custodial symmetry violation can be the couplings of the scalar fields to the $U(1)_X$ gauge boson. We work in the $U(1)_X$ basis where the charges of Φ and H are equal. Changing the $U(1)$ basis shifts the custodial symmetry violation into the gauge kinetic mixing parameter. This happens as the basis change modifies the covariant derivative. In the $B - L$ basis, with a gauge kinetic mixing parameter \tilde{g} ⁵ and the new gauge coupling g_{B-L} , the covariant derivative, restricted to $U(1)$ gauge bosons, acting on

⁴An alternative might be to have a lower scale where custodial symmetry is realized. In this case the SM contribution might be sufficient to trigger EWSB (see also Sec. 6).

⁵Gauge kinetic mixing is often introduced in the kinetic term as $\varepsilon F^{\mu\nu} F'_{\mu\nu}$ [38, 39]. Through basis changes this term can be absorbed into a triangular gauge coupling matrix and the off-diagonal entry is given by $\tilde{g} := \varepsilon g_Y / \sqrt{1 - \varepsilon^2}$ [40].

a generic field ϕ is given by

$$\left[\partial_\mu + i \left(Q^{(Y)}, Q^{(B-L)} \right) \begin{pmatrix} g_Y & \tilde{g} \\ 0 & g_{B-L} \end{pmatrix} \begin{pmatrix} A_\mu^{(Y)} \\ A_\mu^{(X)} \end{pmatrix} \right] \phi. \quad (2.13)$$

$A_\mu^{(Y)}$ and $A_\mu^{(X)}$ are the U(1) gauge fields. Rewriting this in terms of the U(1)_X charge $Q^{(X)}$ defined in Eq. (2.9) yields

$$\left[\partial_\mu + i \left(Q^{(Y)}, Q^{(X)} \right) \begin{pmatrix} g_Y & \tilde{g} - 2q_\Phi g_{B-L} \\ 0 & q_\Phi g_{B-L} \end{pmatrix} \begin{pmatrix} A_\mu^{(Y)} \\ A_\mu^{(X)} \end{pmatrix} \right] \phi. \quad (2.14)$$

We define the kinetic mixing parameter in the new basis as $g_{12} := \tilde{g} - 2q_\Phi g_{B-L}$ and the gauge coupling $g_X := q_\Phi g_{B-L}$. In the presence of fields charged under both U(1) groups, gauge kinetic mixing will generally be generated at the loop level [39] and is therefore non-zero. The difference in the beta functions of λ_p and λ_Φ induced by gauge kinetic mixing is given by

$$\beta_{\lambda_p} - \beta_{\lambda_\Phi} \Big|_{g_{12}} \simeq \frac{g_{12}}{16\pi^2} \left[6g_X^3 + \frac{3}{2}g_{12}g_X^2 \right]. \quad (2.15)$$

In order to ensure that the splitting of λ_Φ and λ_p does not become too large, g_{12} needs to remain small under the RG flow. We find that the choice $q_\Phi = -\frac{16}{41}$ ensures that g_{12} remains zero at one loop if it is set to zero at some initial scale.⁶ This corresponds to the ‘‘charge orthogonality condition’’ [41] (see also [42–44]). In this work we will consider the cases $q_\Phi = -\frac{1}{3}$ and $q_\Phi = -\frac{3}{8}$. For values of $|q_\Phi|$ outside of roughly $|q_\Phi| \in [\frac{1}{3}, \frac{5}{11}]$, g_{12} runs to large values which leads to large contributions in Eq. (2.15) spoiling custodial symmetry. In Fig. 2, we show the flow of g_{12} for the two values of $q_\Phi = -\frac{1}{3}$ (left) and $q_\Phi = -\frac{3}{8}$ (right). In the left plot, g_{12} converges to $g_{12} = \frac{14}{41}g_X$ and in the right plot to $g_{12} = \frac{10}{123}g_X$ (at one loop). In the left plot, we also highlight a trajectory that starts at $g_{12} = 0$ which corresponds to the setup in Sec. 3.1.⁷

For $|g_{12}| \lesssim |g_X|$, the first term in Eq. (2.15) is dominant and the sign of the contribution depends on the relative sign of g_{12} and g_X . If they have the same sign, then Eq. (2.15) leads to $\lambda_p < \lambda_\Phi$ which is required for EWSB.

2.4.3 New Yukawa interactions

If the model includes new fermions with Yukawa couplings to Φ , then these will contribute to $\beta_{\lambda_p} - \beta_{\lambda_\Phi}$ as

$$\beta_{\lambda_p} - \beta_{\lambda_\Phi} \Big|_{y_\psi} \simeq \frac{\sum_k 2y_{\psi_k}^4}{16\pi^2}, \quad (2.16)$$

where we assume real Yukawa couplings. For the model with one new set of fermions the Yukawa interactions are given by Eq. (2.10) and the sum runs over the single value

⁶The value $q_\Phi = -\frac{16}{41}$ was also found in [13, 15].

⁷We stress that the entire analysis of this paper can be done in the $B-L$ basis as long as \tilde{g} is close to $-\frac{2}{3}g_{B-L}$ ($-\frac{3}{4}g_{B-L}$) for $q_\Phi = -\frac{1}{3}$ ($-\frac{3}{8}$) which is equivalent to our model with small g_{12} .

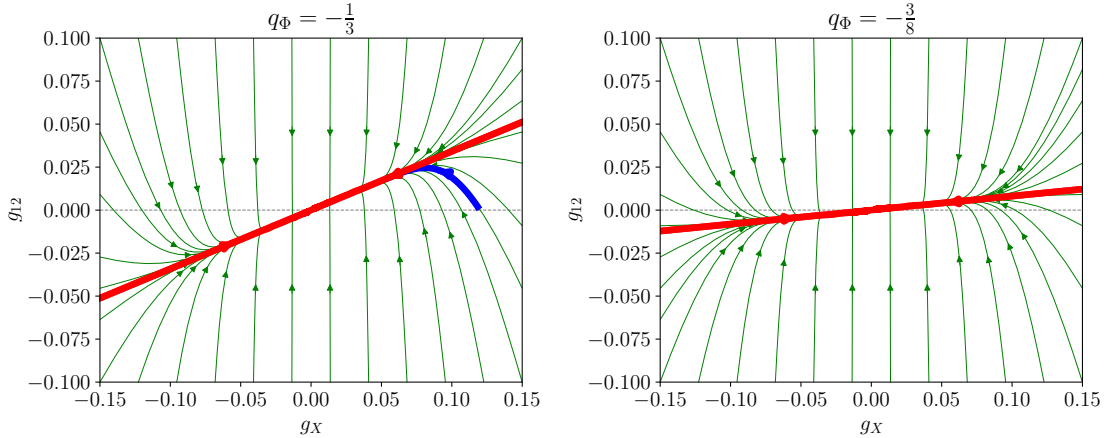


Figure 2. The trajectories of the RG flow in the $g_X - g_{12}$ plane calculated at one loop. The arrows represent the flow from the UV to the infrared (IR). g_Y has been set to 0.48. The red lines correspond to $g_{12} = \frac{14}{41}g_X$ for $q_\Phi = -\frac{1}{3}$ and $g_{12} = \frac{10}{123}g_X$ for $q_\Phi = -\frac{3}{8}$. The blue line highlights a typical trajectory in the minimal model.

$\bar{y}_\psi := \sqrt{y_\psi^\alpha y_\psi^\alpha}$. In the DM model, the Yukawa interactions are given by Eq. (2.11) and the sum runs over y_ψ and $y_{\psi'}$. Such new Yukawa couplings lead to $\lambda_p < \lambda_\Phi$ which is required for EWSB. In the remainder of this work, the sum over k is always understood as running over all Yukawa interaction involving Φ .

2.5 The effective potential

The Coleman-Weinberg potential for background fields Φ_b and H_b at one loop in $\overline{\text{MS}}$ is given by

$$V_{\text{eff}} = V_{\text{tree}} + \sum_i \frac{n_i (-1)^{2s_i}}{64\pi^2} m_{i,\text{eff}}^4 \left[\ln \left(\frac{m_{i,\text{eff}}^2}{\mu^2} \right) - C_i \right], \quad (2.17)$$

where n_i is the number of degrees of freedom for the corresponding field, $(-1)^{2s_i}$ is +1 for bosons and -1 for fermions. C_i is given by $\frac{3}{2}$ for fermions and scalar fields and $\frac{5}{6}$ for vector bosons. The sum runs over all fields present in the respective version of our model. The effective masses $m_{i,\text{eff}}$ for the neutral gauge bosons are given by the eigenvalues of

$$M_V = \begin{pmatrix} \frac{g_Y^2}{2} H_b^2 & -\frac{g_Y g_L}{2} H_b^2 & \frac{(2g_X + g_{12})g_Y}{2} H_b^2 \\ -\frac{g_Y g_L}{2} H_b^2 & \frac{g_L^2}{2} H_b^2 & -\frac{(2g_X + g_{12})g_L}{2} H_b^2 \\ \frac{(2g_X + g_{12})g_Y}{2} H_b^2 & -\frac{(2g_X + g_{12})g_L}{2} H_b^2 & 2 \left(\frac{2g_X + g_{12}}{2} \right)^2 H_b^2 + 2g_X^2 \Phi_b^2 \end{pmatrix}. \quad (2.18)$$

For charged gauge bosons we have $m_{W^\pm, \text{eff}}^2 = \frac{g_L^2}{2} H_b^2$ and for the top quark $m_{t, \text{eff}} = y_t H_b$. The effect of the other SM fermions can be neglected due to their small Yukawa couplings. The scalar effective masses, determined by the second derivative of the tree level potential, are given by $(2\lambda_p \Phi_b^2 + 2\lambda_H H_b^2, 2\lambda_p \Phi_b^2 + 2\lambda_H H_b^2, 2\lambda_p \Phi_b^2 + 2\lambda_H H_b^2, 2\lambda_p H_b^2 + 2\lambda_\Phi \Phi_b^2)$ and the

eigenvalues of

$$\begin{pmatrix} 2\lambda_p H_b^2 + 6\lambda_\Phi \Phi_b^2 & 4\lambda_p H_b \Phi_b \\ 4\lambda_p H_b \Phi_b & 2\lambda_p \Phi_b^2 + 6\lambda_H H_b^2 \end{pmatrix}. \quad (2.19)$$

For the model with one additional set of fermions, there is an additional effective mass given by $m_{\psi,\text{eff}}^2 = y_\psi^\alpha y_\psi^\alpha \Phi_b^2$. In the DM model one needs to include the effective masses $m_{\psi,\text{eff}} = y_\psi \Phi_b$ and $m_{\psi',\text{eff}} = y_{\psi'} \Phi_b$. The values of Φ_b and H_b at the minimum of the Coleman-Weinberg potential are the VEVs $\langle \Phi \rangle$ and $\langle H \rangle$.

Running from the custodially symmetric point at M_{Pl} down to the intermediate scale, the top Yukawa coupling drives λ_H to large positive values. Therefore, the flat direction is mostly aligned with Φ such that $\langle \Phi \rangle \gg \langle H \rangle$ (see Eq. (2.8)). In order to obtain insight into the effect of custodial symmetry violation on the Higgs potential, we will now discuss analytic approximations of the Coleman-Weinberg potential. To this end, we first solve the minimum condition for Φ_b for general H_b and use this to implicitly define $\tilde{\Phi}(H_b)$ via

$$\left. \frac{\partial V_{\text{eff}}}{\partial \Phi_b} \right|_{\Phi_b = \tilde{\Phi}(H_b)} = 0. \quad (2.20)$$

This procedure resembles Effective Field Theory (EFT) methods [45, 46] noting, however, that the CW potential is a function rather than a functional of the constant background fields. The VEV of Φ in the limit $\langle \Phi \rangle \gg \langle H \rangle$ can be approximated by $\Phi_0 := \tilde{\Phi}(H_b = 0)$ which is given by

$$\ln \left(\frac{\Phi_0^2}{\mu^2} \right) = - \frac{16\pi^2 \lambda_\Phi + \left\{ g_X^4 [3 \ln(2g_X^2) - 1] + 4\lambda_p^2 [\ln(2\lambda_p) - 1] - \sum_k \left[y_{\psi_k}^4 (\ln y_{\psi_k}^2 - 1) \right] \right\}}{\left(3g_X^4 + 4\lambda_p^2 - \sum_k y_{\psi_k}^4 \right)}. \quad (2.21)$$

We use the same summation for the Yukawa couplings as in Eq. (2.16). This is the usual result of dimensional transmutation. We now define a new potential for H_b as

$$V_{\text{EFT}}(H_b) := V_{\text{eff}}(H_b, \tilde{\Phi}(H_b)). \quad (2.22)$$

This new potential has a minimum at $H_b = \langle H \rangle$ since

$$\left. \frac{\partial V_{\text{EFT}}}{\partial H_b} \right|_{H_b = \langle H \rangle} = \left. \frac{\partial V_{\text{eff}}}{\partial H_b} + \frac{\partial V_{\text{eff}}}{\partial \Phi_b} \frac{\partial \tilde{\Phi}}{\partial H_b} \right|_{H_b = \langle H \rangle, \Phi_b = \langle \Phi \rangle} = 0, \quad (2.23)$$

where the last equality is true since, by definition, $\langle \Phi \rangle$ and $\langle H \rangle$ fulfill the minimum conditions for V_{eff} . We now expand V_{EFT} in orders of H_b/Φ_0 and find at quadratic order

$$\begin{aligned} V_{\text{EFT}} \supset 2 \left[\lambda_p - \frac{3 \left(g_X + \frac{g_{12}}{2} \right)^2 g_X^2}{3g_X^4 + 4\lambda_p^2 - \sum_k y_{\psi_k}^4} \left(\lambda_\Phi + \sum_k \left\{ \frac{y_{\psi_k}^4}{16\pi^2} \left[\frac{2}{3} + \ln \left(\frac{2g_X^2}{y_{\psi_k}^2} \right) \right] \right\} \right) \right] \Phi_0^2 H_b^2 \\ + \frac{\lambda_p \lambda_H}{16\pi^2} [\dots] \Phi_0^2 H_b^2, \end{aligned} \quad (2.24)$$

where [...] are $\mathcal{O}(1)$ terms suppressed by the $\lambda_p \lambda_H / (16\pi^2)$ prefactor. This expression shows how the different sources of custodial symmetry violation impact the Higgs potential. For

small y_ψ and g_{12} , the quadratic (mass) term for the Higgs field is $\approx 2(\lambda_p - \lambda_\Phi)\Phi_0^2 H_b^2$. Note that the SM custodial symmetry violations (i.e. the top Yukawa and the electroweak gauge contributions) do not show up in this expression completely in line with our discussion in Sec. 2.1.

The RG scale μ should be chosen close to Φ_0 in order to avoid large logarithms. It turns out that a particularly convenient choice is $\mu = \mu_0 := \sqrt{2}g_X\Phi_0 e^{-1/6}$. At this scale $|\lambda_\Phi| \ll |\lambda_p|$ and the quadratic term (i.e. Eq. (2.24)) simplifies to

$$V_{\text{EFT}} \supset 2\lambda_p \left\{ 1 + \frac{[4\lambda_p + 6\lambda_H] \left[\ln \left(\frac{2\lambda_p\Phi_0^2}{\mu_0^2} \right) - 1 \right]}{16\pi^2} \right\} H_b^2 \Phi_0^2. \quad (2.25)$$

Note how this quadratic term, which resembles the Higgs mass term, is $\approx 2\lambda_p\Phi_0^2 H_b^2$ and therefore $\lambda_p\Phi_0^2$ should be of the order of the electroweak scale squared. This agrees with the flat direction in the Gildener-Weinberg approximation, in the sense that Eq. (2.8) implies

$$\lambda_H H^2 = -\lambda_p \Phi^2 \quad (2.26)$$

along the flat direction. While for Eq. (2.24) we expanded in powers of H_b/Φ_0 , we now introduce a new artificial expansion parameter ϵ as

$$\frac{H_b}{\Phi_0} \rightarrow \epsilon \frac{H_b}{\Phi_0}, \quad \lambda_p \rightarrow \epsilon^2 \lambda_p. \quad (2.27)$$

Sending $\epsilon \rightarrow 0$ corresponds to a 't Hooft-Veneziano-like limit [47, 48]

$$\frac{\Phi_0}{H_b} \rightarrow \infty, \quad \frac{\lambda_p}{\lambda_H} \rightarrow 0, \quad \lambda_p \Phi_0^2 = \lambda_H H_b^2 \text{ (fixed)}. \quad (2.28)$$

Expanding Eq. (2.22) in powers of ϵ up to ϵ^4 we find at $\mu = \mu_0$

$$\begin{aligned} V_{\text{EFT}} = & \frac{-3g_X^4 + \sum_k y_{\psi_k}^4}{32\pi^2} \Phi_0^4 + 2\lambda_p \Phi_0^2 H_b^2 + \lambda_H H_b^4 \\ & + \sum_i \frac{n_i (-1)^{2s_i}}{64\pi^2} m_{i,\text{eff}}^4 \left[\ln \left(\frac{m_{i,\text{eff}}^2}{\mu_0^2} \right) - C_i \right] - \frac{3 \left(\frac{g_{12}}{2} + g_X \right)^4 \left(\sum_k y_{\psi_k}^4 \right)}{16\pi^2 \left(3g_X^4 - \sum_k y_{\psi_k}^4 \right)} H_b^4, \end{aligned} \quad (2.29)$$

where the sum over i runs over the effective masses in the SM with a tree level potential of $V_{\text{tree}} = 2\lambda_p\Phi_0^2 H_b^2 + \lambda_H H_b^4$. Eq. (2.29) agrees with the SM effective potential at one loop [49] up to the last term which gives a correction to the Higgs quartic coupling. We note that expanding Eq. (2.22) in ϵ up to ϵ^4 drops terms $\propto \lambda_p^3\Phi_0^4, \lambda_p^2 H_b^2 \Phi_0^2, \lambda_p H_b^4$ when compared to expanding in H_b/Φ_0 up to $(H_b/\Phi_0)^4$.

2.6 Masses and mixing

With the vacuum structure understood, we now turn to the masses of the new particles.

2.6.1 Scalar masses

We calculate the scalar mass matrix by taking the second derivatives of Eq. (2.17), i.e. $m_{ab}^2 = \partial_{\phi_a} \partial_{\phi_b} V_{\text{eff}}$ evaluated at $H_b = \langle H \rangle = v_H/\sqrt{2}$ and $\Phi_b = \langle \Phi \rangle = v_\Phi/\sqrt{2}$. For the dilaton mass we find

$$m_{h_\Phi}^2 \approx \frac{3g_X^4 - \sum_k y_{\psi_k}^4 + 4\lambda_p^2 v_\Phi^2}{4\pi^2} \approx \beta_{\lambda_\Phi} v_\Phi^2. \quad (2.30)$$

The dilaton is the pNGB associated with spontaneous breaking of scale symmetry and the mass is suppressed by the scale anomaly, i.e. the beta function. The mass of the physical Higgs boson is approximated by (at $\mu = \Phi_0$, λ_p is smaller than zero)

$$m_h^2 \approx 2 \left[-\lambda_p + \frac{3(g_X + \frac{g_{12}}{2})^2 g_X^2}{3g_X^4 + 4\lambda_p^2 - \sum_k y_{\psi_k}^4} \left(\lambda_\Phi + \sum_k \left\{ \frac{y_{\psi_k}^4}{16\pi^2} \left[\frac{2}{3} + \ln \left(\frac{2g_X^2}{y_{\psi_k}^2} \right) \right] \right\} \right) \right] v_\Phi^2. \quad (2.31)$$

In the limit of vanishing g_{12} and y_{ψ_k} , this reduces to $m_h^2 \approx 2(\lambda_\Phi - \lambda_p) v_\Phi^2$. The physical Higgs boson is the pNGB associated with spontaneous breaking of SO(6) custodial symmetry and the mass is generated via the differential running of λ_p and λ_Φ . The Higgs-dilaton mixing angle is approximately given by

$$\tan \theta \approx \frac{2 \left[\lambda_p - \frac{3(g_X + \frac{g_{12}}{2})^2 g_X^2}{3g_X^4 + 4\lambda_p^2 - \sum_k y_{\psi_k}^4} \left(\lambda_\Phi + \sum_k \left\{ \frac{y_{\psi_k}^4}{16\pi^2} \left[\frac{2}{3} + \ln \left(\frac{2g_X^2}{y_{\psi_k}^2} \right) \right] \right\} \right) + \frac{3(g_X + \frac{g_{12}}{2})^2 g_X^2}{16\pi^2} \right] v_\Phi v_H}{m_h^2 - m_{h_\Phi}^2} \quad (2.32)$$

and takes values of $\tan \theta \lesssim 10^{-2}$ for typical viable points.

2.6.2 Vector masses

The mass matrix for the neutral gauge bosons M_V is given by Eq. (2.18) evaluated at the VEVs $H_b = \langle H \rangle = v_H/\sqrt{2}$ and $\Phi_b = \langle \Phi \rangle = v_\Phi/\sqrt{2}$. The eigenvalues are obtained by $U^T M_V U$ with

$$U = \begin{pmatrix} c & -sc' & ss' \\ s & cc' & -cs' \\ 0 & s' & c' \end{pmatrix}, \quad (2.33)$$

where $s = \sin(\theta_W)$ and $c = \cos(\theta_W)$ with the electroweak mixing angle $\theta_W = \arctan\left(\frac{g_Y}{g_L}\right)$ and $s' = \sin(\theta')$ and $c' = \cos(\theta')$ with

$$\tan(2\theta') = -\frac{2(g_{12} + 2g_X)\sqrt{g_L^2 + g_Y^2}v_H^2}{[g_L^2 + g_Y^2 - (g_{12} + 2g_X)^2]v_H^2 - 4g_X^2v_\Phi^2}. \quad (2.34)$$

The masses of the Z and Z' bosons are given by

$$m_Z^2 = \frac{1}{2}(g_L^2 + g_Y^2)\frac{v_H^2}{2} \left[1 - \frac{(g_{12} + g_X)^2}{g_X^2} \frac{v_H^2}{v_\Phi^2} + \mathcal{O}\left(\frac{v_H^4}{v_\Phi^4}\right) \right], \quad (2.35)$$

$$m_{Z'}^2 = 2g_X^2\frac{v_\Phi^2}{2} + \frac{1}{2}(g_{12} + 2g_X)^2\frac{v_H^2}{2} + \mathcal{O}\left(\frac{v_H^4}{v_\Phi^4}\right), \quad (2.36)$$

while the photon remains massless. The Z mass is shifted compared to the SM prediction constraining the scale of CW symmetry breaking. However, we will see below that this constraint turns out to be weaker than the limits from direct Z' searches.

3 Different models realizing Custodial Naturalness

3.1 Minimal model

The minimal model that realizes Custodial Naturalness consists of the fields given in Tab. 1 with no additional fermions. We choose $q_\Phi = -\frac{1}{3}$ which is the same setup as in Ref. [26]. In this section we reproduce the main findings and give more details on how custodial symmetry violation in form of gauge kinetic mixing g_{12} affects the hierarchy.

A natural boundary condition for gauge kinetic mixing at M_{Pl} is $g_{12}|_{M_{\text{Pl}}} = 0$, which enhances custodial symmetry at the high scale. With this condition imposed, the model has the same number of free parameters as the SM. Along the RG flow, g_{12} runs towards non-zero values (see Fig. 2) guaranteeing $\lambda_p - \lambda_\Phi < 0$ and therefore EWSB. Allowing for non-zero g_{12} at Planck scale opens up the parameter space.

We explore the parameter space by means of a random scan. In order to find reasonable starting points at M_{Pl} , we sample the input values at the low scale and run these couplings up to the Planck scale where we impose custodial symmetry $\lambda_\Phi|_{M_{\text{Pl}}} = \lambda_p|_{M_{\text{Pl}}} = \lambda_H|_{M_{\text{Pl}}}$. This set of parameters is then run down to μ_0 where we calculate the VEVs and scalar masses before matching to the SM.

More precisely, we choose the top pole mass in the 3σ range $M_t \in [170.4, 174.6]$ GeV. The $\overline{\text{MS}}$ values for the SM gauge and Yukawa couplings are then obtained using the formulae in Ref. [50], while the parameters in the SM Higgs potential (i.e. λ_H^{SM} and m_H^{SM}) are chosen in such a way that the one loop effective potential reproduces the central values of the Higgs VEV and mass at $\mu = M_t$. We then run all couplings up to a randomly chosen scale $\tilde{\mu}_0 \in [500, 10^6]$ GeV using the SM two loop RGEs and choose a random value for $g_X|_{\tilde{\mu}_0} \in [0, 0.20]$. Eq. (2.21) together with $\tilde{\mu}_0 = \sqrt{2}g_X\Phi_0e^{-1/6}$ allows us to derive $\lambda_\Phi|_{\tilde{\mu}_0}$. We also set $\lambda_H|_{\tilde{\mu}_0} = \lambda_H^{\text{SM}}|_{\tilde{\mu}_0}$ and $\lambda_p|_{\tilde{\mu}_0} = \lambda_\Phi|_{\tilde{\mu}_0}$ which are reasonable estimates and the precise values will be set by custodial symmetry at the high scale. With all couplings fixed, we use the two loop RGEs obtained with PyR@TE [51] to run up to M_{Pl} where we impose SO(6) custodial symmetry by the formal replacement $\lambda_H, \lambda_p|_{M_{\text{Pl}}} \rightarrow \lambda$ with $\lambda := \lambda_\Phi|_{M_{\text{Pl}}}$. We choose $g_{12}|_{M_{\text{Pl}}} = 0$ or $g_{12}|_{M_{\text{Pl}}} \in [-0.1, 0.1] \cdot g_X|_{M_{\text{Pl}}}$ for the gauge kinetic mixing parameter. This defines a set of sensible starting parameters at M_{Pl} .

Given a set of couplings at M_{Pl} , we use the two loop RGEs to run down to a new scale μ_0 , which is found by iteratively using Eq. (2.21) as well as the definition of μ_0 . At this scale, we calculate the VEVs and scalar masses numerically from the full effective potential Eq. (2.17). Matching to the SM is done by requiring that the SM effective potential at μ_0 gives the same values for the electroweak VEV and Higgs mass as Eq. (2.17). This allows us to fix the couplings in the SM Higgs potential (i.e. λ_H^{SM} and m_H^{SM}). These couplings are run down to M_t where we calculate the Higgs VEV and mass from the SM effective potential and the top pole mass by inverting the formula in Ref. [50]. We exclude all points

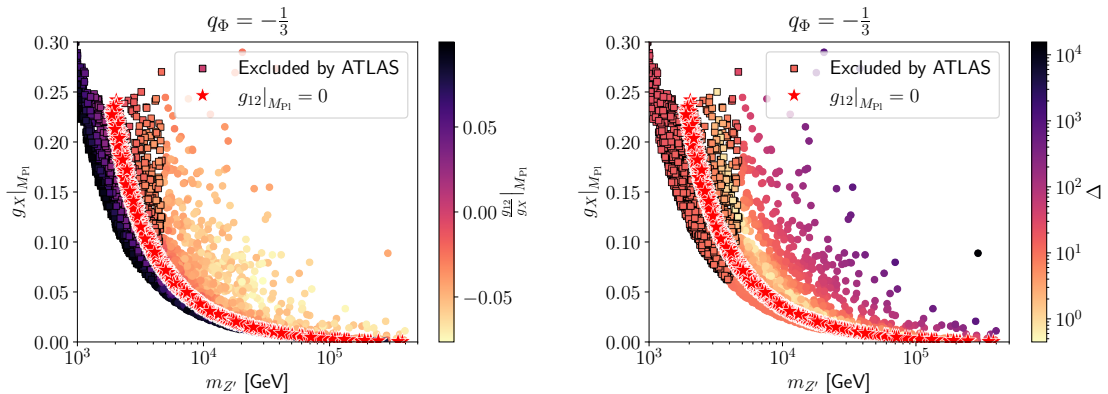


Figure 3. Parameter points that reproduce the correct EW scale in the minimal model. Shown are the custodial symmetry violating parameter g_{12} (left) and the amount of fine tuning (right).

that yield a Higgs VEV outside of $v_H^{\text{exp}} \pm 0.1 \text{ GeV}$. This is the same setup as in Ref. [26] and, in case of the minimal model, also the same data is used. Unless stated otherwise we do not impose a constraint on the Higgs mass. We have checked that the points with correct Higgs mass are roughly evenly distributed in the allowed parameter space.

We show the points that reproduce the correct EW scale in Fig. 3. Points marked by red stars obey $g_{12}|_{M_{P1}} = 0$ and for these points the new physics scale (say, $m_{Z'}$) is set by g_X . Other points have a random value for $g_{12}|_{M_{P1}}$. The input value of g_{12} plays a major role in the hierarchy between the new physics scale and the EW scale (see Fig. 3 (left)). For $g_{12}|_{M_{P1}} \lesssim -0.075 \cdot g_X|_{M_{P1}}$, λ_p would be larger than λ_Φ , implying that no EWSB would occur which excludes this region.

In order to quantify fine tuning, we use a variant of the Barbieri-Giudice measure [52]. We calculate

$$\Delta := \max_{g_i} \left| \frac{g_i}{\langle H \rangle} \frac{\partial \langle H \rangle}{\partial g_i} - \frac{g_i}{\langle \Phi \rangle} \frac{\partial \langle \Phi \rangle}{\partial g_i} \right|. \quad (3.1)$$

The VEVs have a shared sensitivity to the high scale, intrinsic to the mechanism of dimensional transmutation. Our choice of measure in Eq. (3.1) automatically subtracts this common sensitivity, which is not the result of a fine tuning [53], in order to expose the actual tuning required to obtain the hierarchy between $\langle \Phi \rangle$ and $\langle H \rangle$. The derivatives in Eq. (3.1) are calculated numerically by small variations of the input values at M_{P1} . The fine tuning for all points is shown in Fig. 3 (right). For most points, $\Delta \lesssim 10$ demonstrating that our mechanism generates a hierarchy of $\langle H \rangle \approx 10^{-3} \times \langle \Phi \rangle$ without fine tuning. The fine tuning measure also has a minimum where $\Delta \lesssim 1$. Whether there is a physical meaning to this “valley of minimal tuning” is presently unclear. While the order of magnitude for the tuning is independent of the choice of measure, the valley is not. If we calculate the fine tuning for $m_h/\langle \Phi \rangle$ rather than $\langle H \rangle/\langle \Phi \rangle$, then there is no valley.

In order to quantify the strongest direct experimental constraints on this model, we calculate the fiducial cross section times branching ratio for Z' production and decay into

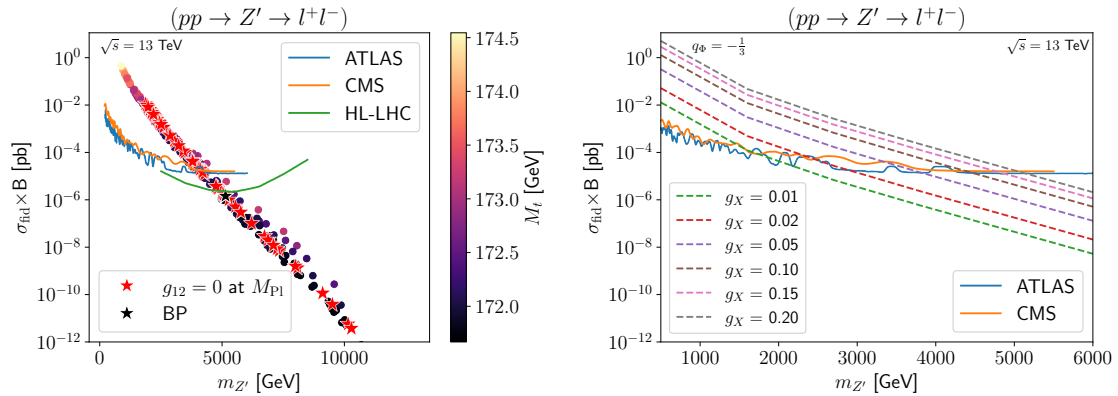


Figure 4. Left: Fiducial cross section times branching ratio ($Z' \rightarrow l^+l^-$ with $l = e, \mu$) for parameter points of the minimal model and 95% C.L. limits from ATLAS and CMS dilepton resonance searches [57, 58] as well as projections for HL-LHC (at 14 TeV) [59]. Only points that reproduce the correct EW scale and Higgs mass are shown. Right: Fiducial cross section times branching ratio for Z' boson with $q_\Phi = -\frac{1}{3}$ for different values of g_X .

two leptons ($l = e, \mu$) using MadGraph5_aMC@NLO [54] with an UFO file [55] obtained using FeynRules [56]. The results, with the same fiducial cuts as in Ref. [57], are shown in Fig. 4 (left). Dilepton resonance searches [57, 58] exclude $m_{Z'} \lesssim 4$ TeV. We recast the limits from Ref. [57] by calculating the fiducial cross section times branching ratio for the Z' boson in our model with different masses and couplings (Fig. 4 (right)). We take the intersections of the lines with fixed g_X and the 95% C.L. exclusion contour of ATLAS [57]. In case of two crossings, we use the lower value. Interpolating these points then allows us to exclude points on the $m_{Z'} - g_X$ plane. The excluded points are marked by black squares in Fig. 3 and the rest of this work. While Fig. 4 shows the results for $q_\Phi = -\frac{1}{3}$, we also do the same calculation with $q_\Phi = -\frac{3}{8}$ to obtain the recasted limits for models with $q_\Phi = -\frac{3}{8}$.⁸

3.2 Minimal fermion extension - Neutrino portal model

Next, we consider a model with the choice $q_\Phi = -\frac{3}{8}$. For this charge assignment, gauge kinetic mixing tends to remain small (see Fig. 2). The minimal setup with $g_{12} = 0$ at the Planck scale does not lead to EWSB since the gauge kinetic mixing remains too small to overcome the SM contributions to $\beta_{\lambda_p} - \beta_{\lambda_\Phi}$ which have the incorrect sign. Therefore, additional sources of custodial symmetry violation are required. The simplest way is to assume $g_{12}|_{M_{\text{Pl}}} > 0$. Alternatively, we can introduce new fermions with a Yukawa coupling to Φ .

The minimal way to introduce new fermions while allowing for a Yukawa interaction involving Φ is shown in Tab. 1 (middle). The new fermions are vector-like⁹ and their

⁸We do not include new fermions in the calculation. These new fermions affect the width of the Z' boson, however the effect is small.

⁹All vector-like mass term are forbidden by scale invariance.

contributions to gauge anomalies cancel. The new Yukawa interaction given in Eq. (2.10) involves ψ_L , Φ and ν_R , connecting the new physics sector to the neutrino portal.

After spontaneous symmetry breaking, the neutral fermions obtain Dirac mass terms given by

$$\mathcal{L}_{\text{mass}} \supset (\bar{\nu}_L^\alpha \bar{\psi}_L) \begin{pmatrix} y_\nu^{\alpha\beta} \frac{v_H}{\sqrt{2}} & 0 \\ y_\psi^\beta \frac{v_\Phi}{\sqrt{2}} & 0 \end{pmatrix} \begin{pmatrix} \nu_R^\beta \\ \psi_R \end{pmatrix} + \text{h.c.} =: (\bar{\nu}_L^\alpha \bar{\psi}_L) M_N \begin{pmatrix} \nu_R^\beta \\ \psi_R \end{pmatrix} + \text{h.c.} \quad (3.2)$$

Majorana mass terms are not generated even at loop level due to an unbroken (accidental) lepton number symmetry. An additional chiral symmetry ensures that ψ_R cannot obtain a mass term. The squared fermion masses are obtained as the eigenvalues of $(\alpha, \alpha' = 1, 2, 3, \text{ a sum over } \beta \text{ is implicit})$

$$M_N M_N^\dagger = \begin{pmatrix} y_\nu^{\alpha\beta} (y_\nu^\dagger)^{\beta\alpha'} \frac{v_H^2}{2} & y_\nu^{\alpha\beta} (y_\psi^*)^\beta \frac{v_H v_\Phi}{2} \\ y_\psi^\beta (y_\nu^\dagger)^{\beta\alpha'} \frac{v_H v_\Phi}{2} & y_\psi^\beta (y_\psi^*)^\beta \frac{v_\Phi^2}{2} \end{pmatrix}. \quad (3.3)$$

For simplicity, we assume real Yukawa couplings. The mass matrix has rank 3 (see Eq. 3.2), i.e. one eigenvalue vanishes. Since $v_\Phi \gg v_H$, the lower right entry dominates and the heavy sterile (with respect to the SM interactions) eigenstate with mass $\approx \sqrt{y_\psi^\beta y_\psi^\beta} \frac{v_\Phi}{\sqrt{2}} = \bar{y}_\psi \frac{v_\Phi}{\sqrt{2}}$, written as a Dirac spinor Ψ , is given by

$$\Psi \sim \begin{pmatrix} \cos(\alpha_\psi) \psi_L + \sin(\alpha_\psi) \nu_L \\ \nu'_R \end{pmatrix}. \quad (3.4)$$

Here, $\sin(\alpha_\psi) \approx y_\nu v_H / (y_\psi v_\Phi)$, which is automatically suppressed thereby justifying the notion as a sterile state, and ν'_R is a linear combination of the right-handed neutrinos (not involving ψ_R). The other two massive eigenstates are active Dirac neutrinos with masses $\sim y_\nu \frac{v_H}{\sqrt{2}}$. The remaining massless state is an active neutrino, i.e. this model predicts that the lightest generation of active neutrinos is massless.

We perform two parameter scans with a setup similar to the minimal model. For the first scan, we assume $\bar{y}_\psi = 0$ and $g_{12}|_{M_{P1}} \in [0, 0.2] \cdot g_X|_{M_{P1}}$ and for the second scan $\bar{y}_\psi|_{\tilde{\mu}_0} \in [0, 0.9] \cdot g_X|_{\tilde{\mu}_0}$ and $g_{12}|_{M_{P1}} = 0$. Fig. 5 shows how the strength of custodial symmetry violation affects the hierarchy, illustrating how small but non-zero values of \bar{y}_ψ or $g_{12}|_{M_{P1}}$ are required to overcome the SM contributions to $\lambda_p - \lambda_\Phi$. Large values of \bar{y}_ψ or $g_{12}|_{M_{P1}}$ lead to more SO(6) custodial symmetry violation and therefore a smaller hierarchy. This is a numerical demonstration of the fact that additional sources of custodial symmetry breaking are needed for successful phenomenology. We also show the amount of fine tuning calculated using Eq. (3.1).

3.3 Dark matter model

We present a simple model that allows for two-component WIMP DM¹⁰ for which we again choose $q_\Phi = -\frac{3}{8}$. Similar to the model in Sec. 3.2, gauge kinetic mixing remains small (see

¹⁰The minimal way to include new stable fermions while canceling the gauge anomalies requires us to introduce two copies. These stable particles form two-component DM meaning that both components will have a non-zero relic density.

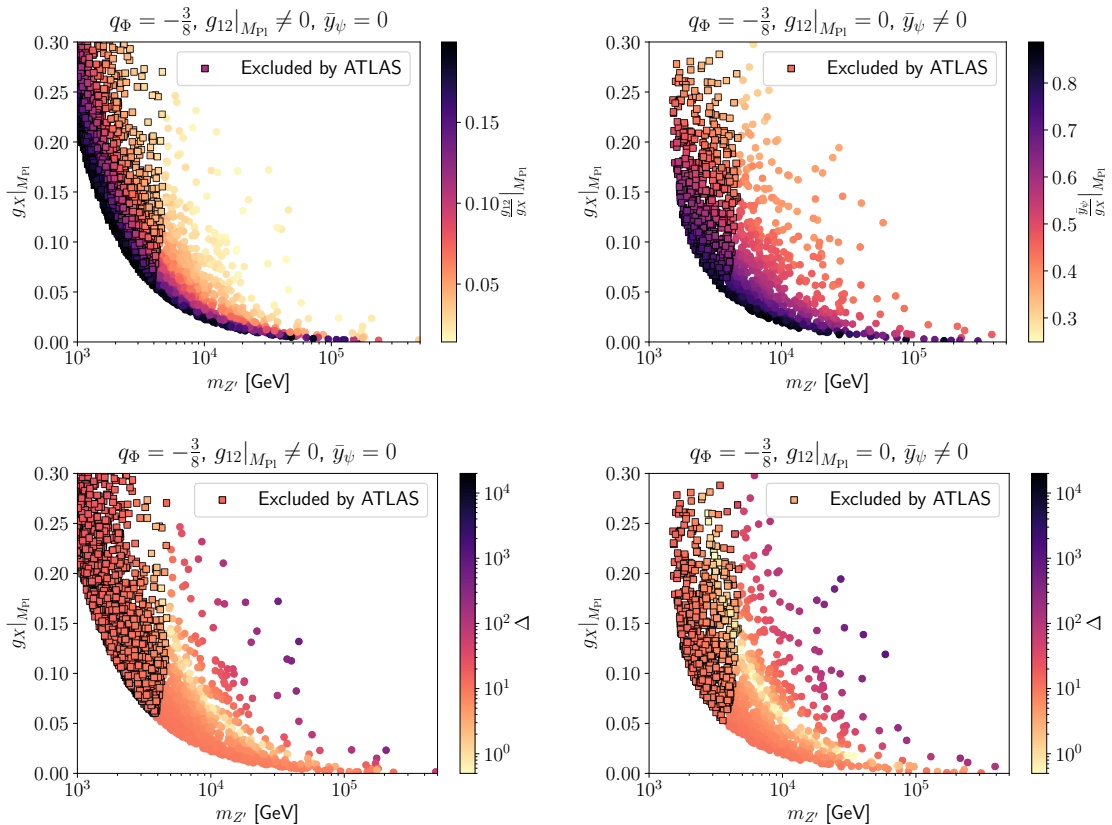


Figure 5. Parameter points that reproduce the correct EW scale in the neutrino portal model with $\bar{y}_\psi^\alpha = 0$ and $g_{12}|_{M_{P1}} \neq 0$ (left) and with $\bar{y}_\psi^\alpha \neq 0$, $g_{12}|_{M_{P1}} = 0$ (right). Shown are the effects of the custodial symmetry violation via g_{12} and \bar{y}_ψ (top) and the amount of fine tuning (bottom).

Fig. 2). We add a pair of vector-like fermions with charges given in Tab. 1 (bottom). The value of p is a free parameter as long as the coupling to the right-handed neutrinos is forbidden. For the numerical analysis we choose $p = \frac{1}{2}$. The new Yukawa interactions are given in Eq. (2.11) and both new Yukawa interactions contribute to custodial symmetry violation. The Lagrangian has two global (accidental) U(1) symmetries under which only the new fermions are charged. Since both of these symmetries remain unbroken after the scalar fields obtain their VEVs, both ψ and ψ' are stable and make up two-component DM. In the early Universe, ψ and ψ' are in thermal equilibrium with the SM and the DM relic density is obtained via a freeze-out process, separately for each of the DM components.¹¹ The total DM relic density Ωh^2 is then given by the sum of the individual relic densities, i.e. $\Omega h^2 = (\Omega h^2)_\psi + (\Omega h^2)_{\psi'}$. The dominant annihilation diagram is the s-channel Z' exchange with SM fermions in the final state (see Fig. 6).

We use the same numerical setup as in the previous sections. We randomly choose

¹¹Thermal equilibrium is only reached if the reheating temperature is high enough which is not necessarily the case in scale invariant models (see e.g. Ref. [60] and our discussion in Sec. 5). A proper analysis of the DM phenomenology requires a detailed analysis of the thermal history of the Universe.

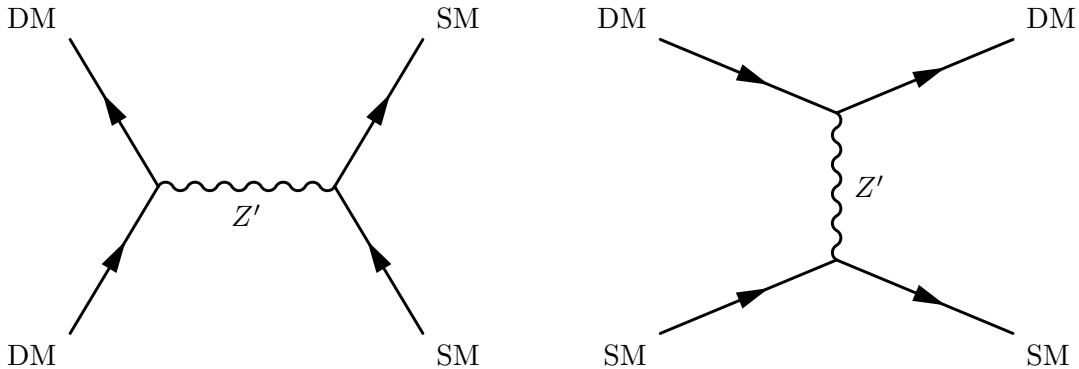


Figure 6. Left: Feynman diagram for dominant DM annihilation channel. The final states are SM fermions. Right: Feynman diagram for the dominant channel contributing to DM-nucleon scattering.

$y_\psi|_{\tilde{\mu}_0} \in [0, 0.8] \cdot g_X|_{\tilde{\mu}_0}$ and for simplicity $y_{\psi'} = y_\psi$. We perform two parameter scans, one with $g_{12}|_{M_{\text{Pl}}} = 0$ and the second one uses $g_{12}|_{M_{\text{Pl}}} = -0.1 \cdot g_X|_{M_{\text{Pl}}}$. In the second case, g_{12} and $y_\psi, y_{\psi'}$ have opposite contributions to $\lambda_p - \lambda_\Phi$, thereby allowing for larger values of $m_\psi/m_{Z'}$. The effect of custodial symmetry violation from $y_\psi = y_{\psi'}$ and the fine tuning is shown in Fig. 7 (top and middle). The fine tuning for the parameter points with $g_{12}|_{M_{\text{Pl}}} = -0.1 \cdot g_X|_{M_{\text{Pl}}}$ is slightly larger than for $g_{12}|_{M_{\text{Pl}}} = 0$ since gauge kinetic mixing partially cancels the effects of y_ψ and $y_{\psi'}$ and this cancellation requires tuning. We calculate the DM relic density using `micrOMEGAs` 6.0.5 [62] with model files generated using `SARAH-4.15.2` [63]. The results for the relic density are shown in Fig. 7 (bottom). For large parts of the parameter space, the relic density is too large. However, near the Z' resonance $m_\psi \approx m_{\psi'} \approx \frac{1}{2}m_{Z'}$, the annihilation rate is sufficiently large and the relic density can reach the observed or smaller values. Note that $y_\psi \approx y_{\psi'}$, up to deviations of a few percent, is required so that both DM candidates can be near the Z' resonance simultaneously.¹² For $g_{12}|_{M_{\text{Pl}}} = 0$ most of the points that do not overproduce DM are excluded by the ATLAS searches. Only a very small region in parameter space is not excluded by these constraints. Negative values for $g_{12}|_{M_{\text{Pl}}}$ allow for higher Z' masses while not overproducing DM. Points that yield the correct relic abundance lie on the boundary of the region with $\Omega h^2 < 0.12$. Our DM candidates can scatter off nuclei via a virtual Z' exchange (see Fig. 6). We calculate the direct detection cross section using `micrOMEGAs` 6.0.5. Both, ψ and ψ' have the same cross section (assuming $m_\psi = m_{\psi'}$) and the results for the spin independent scattering cross section $\sigma_{\text{SI}} = \sigma_{\text{SI}}(\psi) = \sigma_{\text{SI}}(\psi')$ are shown in Fig. 8. Current direct detection limits turn out to be weaker than the ATLAS limits on the Z' boson. Future direct detection experiments such as DARWIN will reach the neutrino floor and probe parts of our parameter space [66]. More detailed analyses of fermionic DM models with a massive Z' portal can be found e.g. in Refs. [67–72].

¹² $y_\psi = y_{\psi'}$ can be justified by a parity-type symmetry that maps $\psi_L \leftrightarrow \psi'_R$ and $\psi'_L \leftrightarrow \psi_R$.

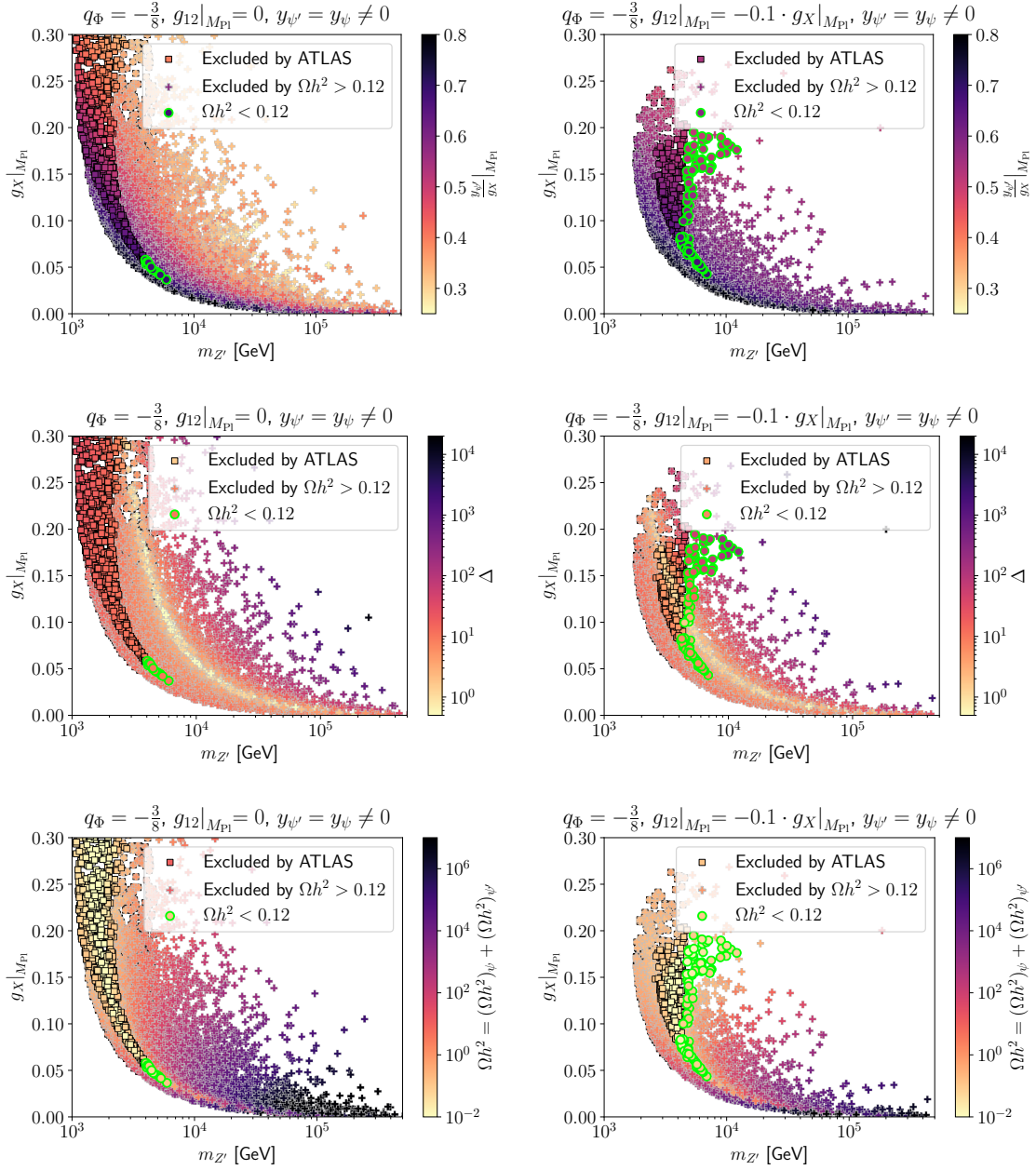


Figure 7. Parameter points for the DM model which reproduce the correct EW scale assuming $g_{12}|_{M_{Pl}} = 0$ (left) and $g_{12}|_{M_{Pl}} = -0.1 \cdot g_X|_{M_{Pl}}$ (right). The two Yukawa couplings are, for simplicity, chosen as $y_{\psi'} = y_{\psi}$. Shown are the effects of custodial symmetry violation via y_{ψ} and $y_{\psi'}$ (top), the fine tuning (middle) and the DM relic density (bottom). Points that yield a DM relic density above the observed value of $\Omega h^2 = 0.12$ [61] are excluded and marked as gray bordered plus symbols while points that yield $\Omega h^2 < 0.12$, and are not excluded by the ATLAS dilepton resonance searches, are marked with bright green bordered points.

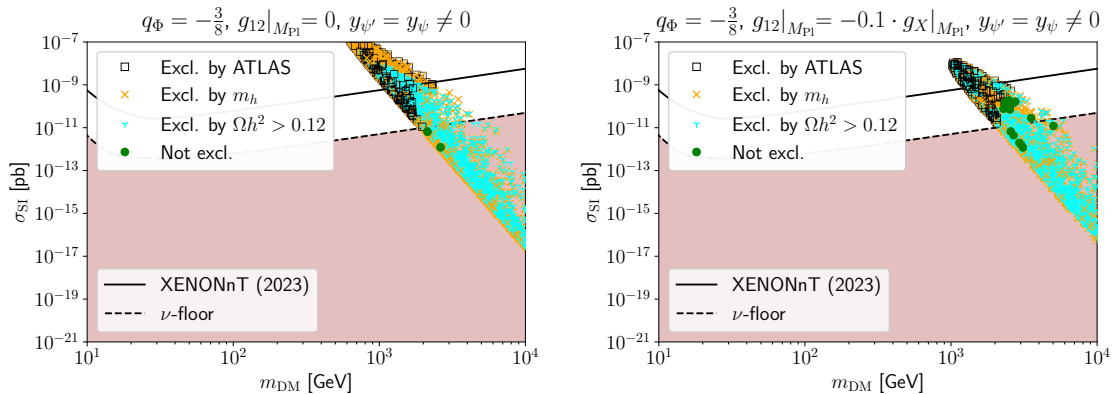


Figure 8. Spin independent (SI) cross section for WIMP-nucleon scattering and XENONnT limits [64]. Also shown is the neutrino floor for Xenon [65]. Black squares indicate points excluded by the ATLAS dilepton resonance searches, orange crosses indicate points where the Higgs mass is outside of its 3σ range, and cyan “tri-down” points indicate points with a DM relic abundance $\Omega h^2 > 0.12$. Phenomenologically viable points are labeled by green dots.

4 New particle masses and further experimental signatures

The experimental uncertainty of the top quark mass turns out to be the major limitation for more precise predictions in our model. This is because the top Yukawa coupling gives the leading contribution to β_{λ_H} and the uncertainty, amplified by the running over many orders of magnitude, translates to an uncertainty on the theoretical prediction of the Higgs mass. We show the relation between the numerical values of the top pole mass M_t and the Higgs mass in Fig. 9 for all points not excluded by the ATLAS dilepton resonance searches. The results are similar for all models studied in this work. The majority of points with the correct Higgs mass also require the top mass to be in its 1σ range with only very few points reaching the upper end of its 3σ allowed interval. In the minimal setup with $q_\Phi = -\frac{1}{3}$ and $g_{12}|_{M_{P1}} = 0$ (white bordered stars), there is an approximately linear relation between the top mass and the Higgs mass. While this setup has the same number of free parameters as the SM, one would need to measure the top mass with 0.1 GeV precision in order to accurately predict the value of $m_{Z'}$. With higher precision on M_t , it might become necessary to calculate the effective potential as well as the RGEs at higher loop order. In the DM model, only few points obey $\Omega h^2 < 0.12$ (dark bordered points) and these few points seem to have the same distribution as the points with no constraint on the relic density. For all models, there are no viable points with $M_t \lesssim 171.5$ GeV. In general, measuring the top quark mass more precisely is an important check for Custodial Naturalness.

The particle spectrum of Custodial Naturalness includes the dilaton with a mass suppressed by the beta-function β_{λ_Φ} (see Eq. (2.30)). We show the values for m_{h_Φ} in Fig. 10. In the minimal scenario with $q_\Phi = -\frac{1}{3}$ and $g_{12}|_{M_{P1}} = 0$ (red stars), the dilaton mass is always smaller than the Higgs mass and approximately 70 GeV with only a small dependence on the intermediate scale $\langle \Phi \rangle$. For models with vanishing y_ψ the dilaton mass is bounded

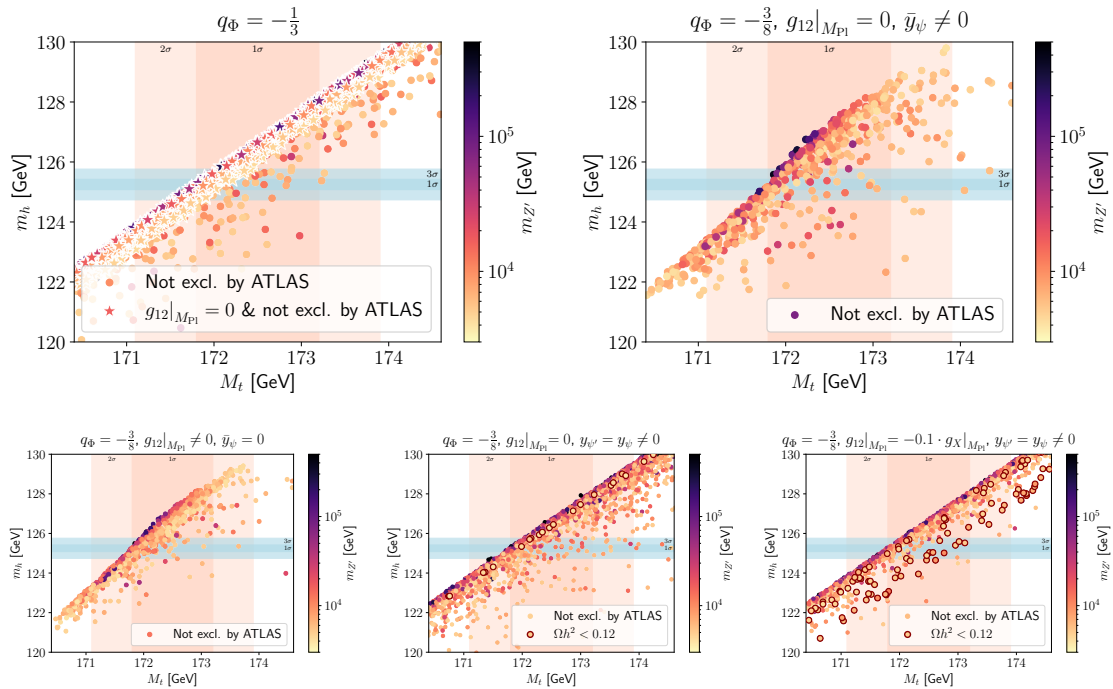


Figure 9. Correlation of the top pole mass M_t and the Higgs mass m_h for the minimal model (top left), the neutrino portal model with $y_\psi \neq 0$, $g_{12}|_{M_{P1}} = 0$ (top right) and with $y_\psi \neq 0$, $g_{12}|_{M_{P1}} \neq 0$ (bottom left) and for the DM model with $g_{12}|_{M_{P1}} = 0$ (bottom middle) and with $g_{12}|_{M_{P1}} = -0.1 \cdot g_X|_{M_{P1}}$ (bottom right) for points that are not excluded by current ATLAS dilepton resonance searches. For the DM model, points that fulfill $\Omega h^2 < 0.12$ are indicated by dark bordered points.

from below by $m_{h_\Phi} \gtrsim 40$ GeV, while for $y_\psi \neq 0$ smaller values are possible only limited by the numerical range of y_ψ . In either case, the dilaton mass can reach up to a few 100 GeV. Points that allow for the correct Higgs mass are evenly distributed.

Numerical values for the Higgs-dilaton mixing angle are shown in Fig. 11. The mixing is suppressed by the heavy scale (see Eq. (2.32)) and for points not excluded by ATLAS, the mixing is typically $\sin^2 \theta \lesssim 10^{-5}$ and, therefore, well below the direct experimental limits on the mixing angle [73–75]. In the degenerate scenario $m_{h_\Phi} \approx m_h$ the mixing can be larger (see also Eq. (2.32)). The couplings of the dilaton to the SM induced by mixing are obtained by SM operators containing h_Φ rather than h , i.e. $\mathcal{O}_{h_\Phi} \approx \sin \theta \times \mathcal{O}_{h \rightarrow h_\Phi}^{\text{SM}}$. Additional couplings of the dilaton to pairs of gauge bosons originate from the trace anomaly, but are suppressed by h_Φ/v_Φ [76–78]. Generic constraints on dilatons, hence, are avoided due to the large value of v_Φ [79, 80], and the dilaton decay branching ratios are, to a good approximation, those of a SM Higgs with the mass of the dilaton. We estimate that, at a Higgs factory, for $\sin^2 \theta \sim \mathcal{O}(10^{-5})$, there would roughly be one dilaton produced per 10^5 Higgs bosons and decay with a lifetime of $\tau_{h_\Phi \rightarrow \text{SM}} \sim \mathcal{O}(10^{-17} \text{ s})$. While a smaller mixing angle would further decrease the dilaton production yield, it would also lead to an increased dilaton lifetime. For long enough dilaton lifetimes, this would open a very

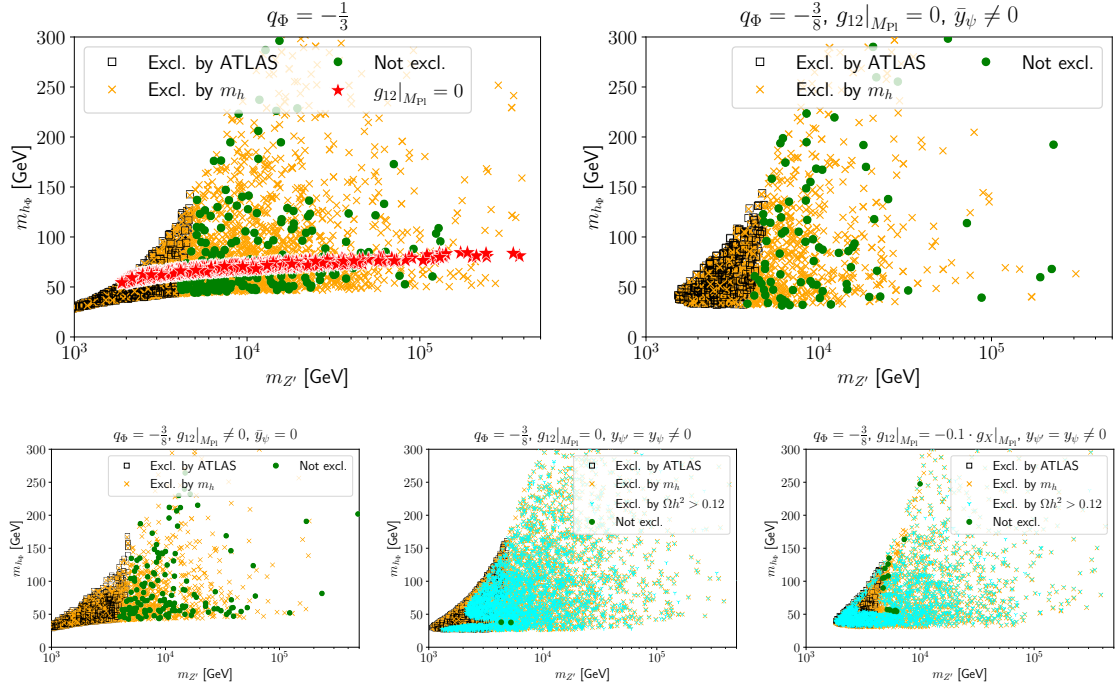


Figure 10. Numerical values of the dilaton mass m_{h_Φ} for the minimal model (top left), the neutrino portal model with $y_\psi \neq 0$, $g_{12}|_{M_{P1}} = 0$ (top right) and with $y_\psi \neq 0$, $g_{12}|_{M_{P1}} = 0$ (bottom left) and for the DM model with $g_{12}|_{M_{P1}} = 0$ (bottom middle) and with $g_{12}|_{M_{P1}} = -0.1 \cdot g_X|_{M_{P1}}$ (bottom right). The black squares indicate points excluded by the ATLAS dilepton resonance searches and the orange crosses indicate points where the Higgs mass is outside of its 3σ range. The green points are not excluded. For the DM model, the cyan “tri-down” points indicate the region where the relic abundance is $\Omega h^2 > 0.12$.

prominent signature in displaced vertex tracking at Higgs factories. For example, for $\sin^2\theta \sim \mathcal{O}(10^{-7})$, 10^7 Higgs bosons would be enough to yield a displaced vertex signature for a dilaton decay if $\mathcal{O}(\mu\text{m})$ vertex tracker resolution could be achieved [81] (see also [82]). Searches of this kind would also benefit from the primary vertex boost inherent to recently proposed asymmetrical beam configurations called HALHF [83, 84].

There would also be additional rare decays of the Higgs boson, or “dilaton strahlung”¹³ emitted from virtual Higgses. The three-scalar vertices, approximated for small custodial symmetry violation ($g_{12} \ll 1$, $y_\psi \ll 1$ and $\lambda_\Phi - \lambda_p \ll 1$), are given by

$$\frac{\partial^3 V_{\text{eff}}}{\partial h^3} \approx 6\lambda_H v_H, \quad (4.1)$$

$$\frac{\partial^3 V_{\text{eff}}}{\partial h^2 \partial h_\Phi} \approx (m_{h_\Phi}^2 - m_h^2) \frac{1}{v_\Phi}, \quad (4.2)$$

$$\frac{\partial^3 V_{\text{eff}}}{\partial h \partial h_\Phi^2} \approx (3m_{h_\Phi}^2 - m_h^2) \frac{v_H}{v_\Phi^2}, \quad (4.3)$$

¹³AT is grateful to Ian M. Lewis for drawing our attention to this process.

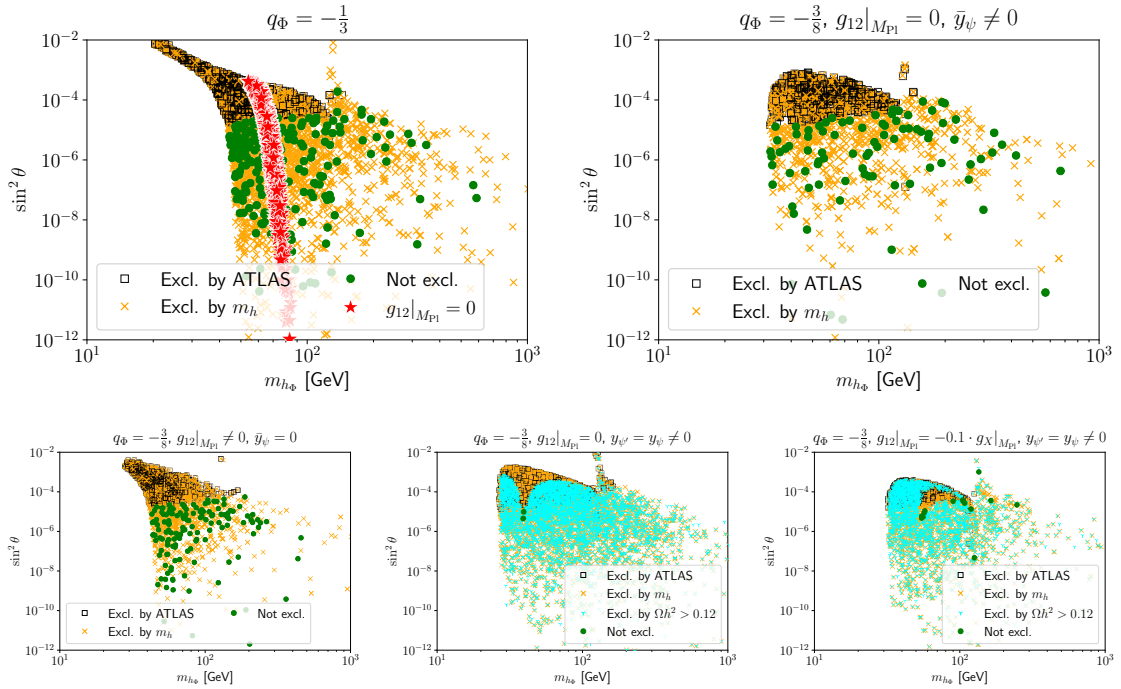


Figure 11. Numerical values for the Higgs-dilaton mixing angle θ as a function of the dilaton mass m_{h_Φ} for the minimal model (top left), the neutrino portal model with $y_\psi \neq 0$, $g_{12}|_{M_{P1}} = 0$ (top right) and with $y_\psi \neq 0$, $g_{12}|_{M_{P1}} = 0$ (bottom left) and for the DM model with $g_{12}|_{M_{P1}} = 0$ (bottom middle) and with $g_{12}|_{M_{P1}} = -0.1 \cdot g_X|_{M_{P1}}$ (bottom right). The black squares indicate points excluded by the ATLAS dilepton resonance searches and the orange crosses indicate points where the Higgs mass is outside of its 3σ range. The green points are not excluded. For the DM model, the cyan “tri-down” points indicate the region where the relic abundance is $\Omega h^2 > 0.12$.

implying that Higgs decays into dilatons, if kinematically allowed, are highly suppressed with a branching fraction of $\Gamma_{h \rightarrow h_\Phi h_\Phi} / \Gamma_{h, \text{tot}} \sim \mathcal{O}(10^{-8})$ and also dilaton strahlung is suppressed by the small mixing angle.

Since Custodial Naturalness is based on new sources of custodial symmetry violation, also electroweak precision tests (EWPT) provide meaningful constraints on our models. To a first approximation, the new sources of custodial breaking induce a shift of the mass of the Z boson visible in Eq. (2.35). If all other couplings keep their SM values, m_Z would stay within its 2σ uncertainty [85] if $\langle \Phi \rangle \gtrsim 18$ TeV. This constraint is always superseded by direct limits on the Z' mass, see Figs. 3, 4, and 5, which justifies our simplistic treatment here. For a detailed analysis, a new global fit to the wealth of EWPT data would be in order, since it can also explore additional parameter correlations in our class of models. This is, however, beyond the scope of this paper.

Finally, The Z' boson can be searched for at future colliders and we show the reach of different proposals in Fig. 12. The projected future limits are taken from Ref. [86, Fig. 8.3] but have been calculated for a hypercharge universal Z' . A more detailed analysis can be done, taking into account the non-universal Z' couplings in our model but results do not

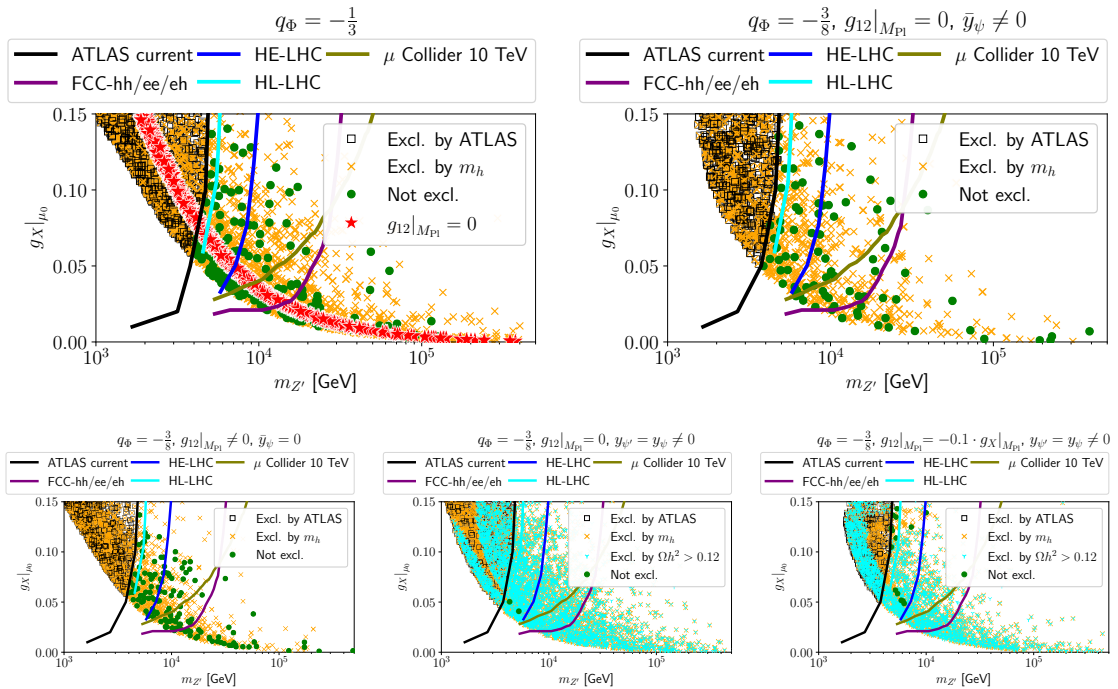


Figure 12. $U(1)_X$ gauge coupling at the matching scale μ_0 vs. $m_{Z'}$ for the minimal model (top left), the neutrino portal model with $y_\psi \neq 0$, $g_{12}|_{M_{P1}} = 0$ (top right) and with $y_\psi \neq 0$, $g_{12}|_{M_{P1}} = 0$ (bottom left) and for the DM model with $g_{12}|_{M_{P1}} = 0$ (bottom middle) and with $g_{12}|_{M_{P1}} = -0.1 \cdot g_X|_{M_{P1}}$ (bottom right). The black squares indicate points excluded by the ATLAS dilepton resonance searches and the orange crosses indicate points where the Higgs mass is outside of its 3σ range [85]. The green points are not excluded. For the DM model, the cyan “tri-down” points indicate the region where the relic abundance is $\Omega h^2 > 0.12$. We also show the recast ATLAS limits [57] and projections for future colliders taken from Ref. [86]. The projections assume a hypercharge universal Z' .

vary by more than an $\mathcal{O}(1)$ factor. For the DM model, all points found in our scans can be excluded by Z' searches at future colliders. Smaller values of $g_{12}|_{M_{P1}}$ than the ones considered here help to escape such searches but would require fine tuning of gauge kinetic mixing against Yukawa couplings.

5 Cosmological evolution and gravitational wave signatures

In this work we have only considered the zero temperature effective potential. Future work should investigate finite temperature effects in the class of Custodial Naturalness models. Coleman-Weinberg type models generically have a first order phase transition (FOPT) [3, 87, 88]. The thermal history of the classically conformal $B-L$ model has been studied for example in Refs. [89–93] and connections to potentially realistic scenarios of Baryo- or Leptogenesis (sometimes also including the production of DM) have been made in Refs. [60, 94–100]. We briefly summarize the main findings. The conformal $B-L$ model differs from our model by the usually considered charge assignment $q_\Phi = 2$ and the fact

that $\text{SO}(6)$ custodial symmetry is not realized. The different charge of Φ can largely be compensated by rescaling the gauge coupling. Note that the qualitative behavior also holds for different values of gauge kinetic mixing [91].

At sufficiently high temperature T , the minimum of the potential is $(\Phi, H) = (0, 0)$. Once the temperature drops, the potential develops a non-trivial minimum. Below the critical temperature $T_c \sim m_{Z'}$, this non-trivial minimum has lower energy than the false vacuum $\Phi = 0$. As a consequence of classical scale invariance, there is always a thermal barrier which does not disappear at low temperature and Φ remains trapped at $\Phi = 0$. The field Φ will tunnel to the non-trivial vacuum leading to the formation of bubbles. However, the percolation temperature T_p where the formation and expansion of bubbles becomes efficient is much lower than the critical temperature $T_p \ll T_c$. This leads to a period of thermal inflation and the number of e -folds for the parameters of our model is typically $N \sim 10$ [91]. It turns out that for large parts of the parameter space, percolation remains inefficient even for temperatures below the QCD scale. Ref. [90] found that in the $B - L$ model this happens if $g_{B-L} \lesssim 0.2$ at $\mu = m_{Z'}$. Rescaling this number as the conformal $B - L$ model corresponds to $q_\Phi = 2$, we find that for our model this bound translates to $g_X \lesssim 0.4$. In this case, the QCD phase transition occurs before $B - L$ symmetry breaking. QCD with $N_f = 6$ massless quarks has a FOPT with a critical temperature $T_c^{\text{QCD}} \approx 85 \text{ MeV}$ [101, 102]. The top quark condensate generates a linear term in the Higgs potential which in turn induces a VEV for the Higgs boson given by $v_{H,\text{QCD}} = |y_t/(\sqrt{2}\lambda_H)\langle t\bar{t}\rangle|^{1/3} \approx 100 \text{ MeV}$ [90, 93]. For the parameter space of our model, Ref. [90] finds that Φ initially remains trapped at $\Phi = 0$ and transitions to the true vacuum by a FOPT. Ref. [93] suggests that a QCD induced tachyonic instability leads to $B - L$ breaking without another FOPT. In both cases, bubble collisions lead to gravitational wave signal and parts of the parameter space can be probed by future gravitational wave observatories [89–93, 97, 98, 103–105].

Future work also should investigate the reheating process. If $m_{h_\Phi} > 2m_h$, which only holds in a small part of our parameter space, then the decay $h_\Phi \rightarrow hh$ reheats the thermal bath and the reheating temperature $T_{\text{rh}} \sim \mathcal{O}(\text{TeV})$ [93]. For most of our parameter space, $m_{h_\Phi} < 2m_h$. Reheating might still be possible, for example through scalar mixing [106].

Altogether this shows that the cosmological history of our model can be realistic, and that the model can be probed by its gravitational wave signal. More detailed investigations are necessary, however, in order to work out reliable quantitative predictions for the specific class of models realizing Custodial Naturalness.

6 Variations and embeddings of Custodial Naturalness

We have shown that the most minimal version of Custodial Naturalness [26] is phenomenologically stable under variations of high-scale boundary conditions and can easily be extended by additional new fermions to incorporate neutrino mass generation and/or fermionic DM candidates. In the present study, we have focused on what we think is the most interesting region of parameter space where custodial symmetry is restored around $\mu \sim M_{\text{Pl}}$. Similar to the SM, this class of models feature a Higgs vacuum in- or better meta-

stability at scales around $\mu \sim 10^{15} - 10^{17}$ GeV, which could be avoided by the introduction of additional fermions (see e.g. Refs. [13–15]). On the other hand, vacuum meta-stability may not be something that needs to be “cured” but could also be an important feature of Nature [107], where scale generation and separation is related to an interacting UV fixed point (see e.g. Ref. [108]) with custodially symmetric quantum critical values of the scalar self-couplings.

A totally different but likewise valid possibility is that the scale of custodial symmetry violation is lowered to $\mu \approx 10^{11}$ GeV, as already remarked in footnote 4. If the scale of custodial symmetry violation is reduced, then SM contributions to $\beta_{\lambda_p} - \beta_{\lambda_\Phi}$ can be sufficiently large to trigger EWSB without requiring additional sources of custodial symmetry breaking. Specifically, for the charge assignment $q_\Phi = -\frac{16}{41}$, g_{12} remains zero at one loop and does not contribute to custodial symmetry violation. Special charge assignments like this could be justified if the $U(1)_X$ together with the SM gauge group should be embedded into a larger simple group similar to a grand unified theory (GUT). The enhanced $SO(6)$ custodial symmetry then might be embedded similarly to the SM custodial symmetry $SO(4) \subset SO(10)$ in Pati-Salam unification [109].

While we have exclusively considered family universal $U(1)_X$ assignments in this work, extensions of the idea of Custodial Naturalness to non-family-universal charge assignments could extend our mechanism of scale separation to the flavor structure of the SM. Extensions such as $B - L$ with charge assignment of right-handed neutrinos $\nu_R \sim (-4, -4, 5)$ could explain the smallness of neutrino masses [110–113], while a charge assignment consistent with $U(1)_{L_\mu - L_\tau}$ might allow an explanation of the observed discrepancy in the muon anomalous magnetic moment [114–119].

Finally, it may also be interesting to investigate scenarios in which spontaneous scale generation is linked to inflation [120, 121], where in our case Φ would have to play the role of the inflaton, see e.g. Refs. [106, 122, 123].

7 Conclusions

We have introduced Custodial Naturalness which is a new mechanism to address the hierarchy problem. The large separation between the Planck scale and a new intermediate scale is generated via dimensional transmutation. The further suppression of the EW scale is naturally explained by the fact that the Higgs boson is a pNGB of an enhanced custodial symmetry that is spontaneously broken at the intermediate scale.

The scalar sector consist of the SM Higgs field and a complex scalar singlet, both of which have identical charges under a new gauged $U(1)$ symmetry. At some high scale, which we take to be the Planck scale, the potential is assumed to be scale invariant and invariant under a $SO(6)$ custodial symmetry. An intermediate scale is generated via the Coleman-Weinberg mechanism, spontaneously breaking scale and custodial symmetry. The Higgs boson is identified as a pNGB associated with the spontaneous breaking of custodial symmetry, therefore avoiding the little hierarchy problem. In our analytical discussion we investigated the impact of explicit custodial symmetry breaking on the Higgs mass. The leading contributions are found to come from gauge kinetic mixing and the Yukawa cou-

plings of potential new fermions while the SM gauge and Yukawa couplings only contribute in a subleading manner.

The minimal realization of Custodial Naturalness consists of the SM extended by a complex scalar singlet and a new $U(1)_X$ gauge symmetry. With the boundary condition of vanishing gauge kinetic mixing at the Planck scale, this model is predictive because it has the same number of parameters as the SM. We have shown that the Custodial Naturalness mechanism is stable under the inclusion of additional fields and new sources of custodial symmetry violation. The minimal fermionic extension connects the new sector to the neutrino portal and predicts two massive Dirac neutrinos, an exactly massless lightest active neutrino, as well as a heavy sterile Dirac neutrino. We also presented a model which naturally encompasses two-component DM and the relic abundance reaches the observed value in a small part of the parameter space which requires some tuning between mass of the heavy vector boson Z' mediator and the DM fermion masses. Both models allow for new Yukawa interactions which violate custodial symmetry and, therefore, indirectly contribute to the Higgs mass. For each model we demonstrated how custodial symmetry violation impacts the hierarchy between the EW and the intermediate scale and we showed, using a variation of the Barbieri-Giudice measure, that our mechanism does not require fine tuning.

The realizations of Custodial Naturalness considered here predict a heavy Z' boson in the 4 – 100 TeV mass range with couplings to all SM fields. Future colliders can probe large parts of the allowed parameter space. If there is no additional tuning, the entire parameter space of the DM model can be tested by future Z' searches. The Dilaton, which is the pNGB associated with spontaneous breaking of scale symmetry, typically has a mass in the 30 – 1000 GeV range, small mixing with the SM Higgs boson, and potentially long enough lifetime to provide a benchmark case for displaced vertex searches at future Higgs factories. For most of the parameter space, the top pole mass is required to be at the lower end of its currently experimentally allowed 1σ range.

The thermal history of the Universe for models similar to ours (i.e. with scale invariance and a similar particle content) has been studied in previous works. Such settings typically feature a strongly supercooled first-order phase transition which gives rise to potentially observable gravitational wave signals. Details of the cosmological evolution in our models and the implications for gravitational wave observatories should be investigated in future work.

Variations of our minimal scenarios can connect the idea of Custodial Naturalness to the flavor structure of the SM while embeddings in unified theories can further constrain the possible charge assignments and may provide insights about the origin of high scale custodial symmetry.

Acknowledgments

The work of AT was partially supported by the Portuguese Fundação para a Ciência e a Tecnologia (FCT) through project 2023.06787.CEECIND and contract 2024.01362.CERN, partially funded through POCTI (FEDER), COMPETE, QREN, PRR, and the EU.

References

- [1] W.A. Bardeen, *On naturalness in the standard model*, in *Ontake Summer Institute on Particle Physics*, 8, 1995.
- [2] S.R. Coleman and E.J. Weinberg, *Radiative Corrections as the Origin of Spontaneous Symmetry Breaking*, *Phys. Rev. D* **7** (1973) 1888.
- [3] S. Weinberg, *Mass of the Higgs Boson*, *Phys. Rev. Lett.* **36** (1976) 294.
- [4] E. Gildener and S. Weinberg, *Symmetry Breaking and Scalar Bosons*, *Phys. Rev. D* **13** (1976) 3333.
- [5] R. Hempfling, *The Next-to-minimal Coleman-Weinberg model*, *Phys. Lett. B* **379** (1996) 153 [[hep-ph/9604278](#)].
- [6] K.A. Meissner and H. Nicolai, *Conformal Symmetry and the Standard Model*, *Phys. Lett. B* **648** (2007) 312 [[hep-th/0612165](#)].
- [7] J.R. Espinosa and M. Quiros, *Novel Effects in Electroweak Breaking from a Hidden Sector*, *Phys. Rev. D* **76** (2007) 076004 [[hep-ph/0701145](#)].
- [8] W.-F. Chang, J.N. Ng and J.M.S. Wu, *Shadow Higgs from a scale-invariant hidden $U(1)(s)$ model*, *Phys. Rev. D* **75** (2007) 115016 [[hep-ph/0701254](#)].
- [9] R. Foot, A. Kobakhidze and R.R. Volkas, *Electroweak Higgs as a pseudo-Goldstone boson of broken scale invariance*, *Phys. Lett. B* **655** (2007) 156 [[0704.1165](#)].
- [10] R. Foot, A. Kobakhidze, K.L. McDonald and R.R. Volkas, *Neutrino mass in radiatively-broken scale-invariant models*, *Phys. Rev. D* **76** (2007) 075014 [[0706.1829](#)].
- [11] S. Iso, N. Okada and Y. Orikasa, *Classically conformal $B-L$ extended Standard Model*, *Phys. Lett. B* **676** (2009) 81 [[0902.4050](#)].
- [12] S. Iso, N. Okada and Y. Orikasa, *The minimal $B-L$ model naturally realized at TeV scale*, *Phys. Rev. D* **80** (2009) 115007 [[0909.0128](#)].
- [13] S. Oda, N. Okada and D.-s. Takahashi, *Classically conformal $U(1)'$ extended standard model and Higgs vacuum stability*, *Phys. Rev. D* **92** (2015) 015026 [[1504.06291](#)].
- [14] A. Das, N. Okada and N. Papapietro, *Electroweak vacuum stability in classically conformal $B-L$ extension of the Standard Model*, *Eur. Phys. J. C* **77** (2017) 122 [[1509.01466](#)].
- [15] A. Das, S. Oda, N. Okada and D.-s. Takahashi, *Classically conformal $U(1)'$ extended standard model, electroweak vacuum stability, and LHC Run-2 bounds*, *Phys. Rev. D* **93** (2016) 115038 [[1605.01157](#)].
- [16] D.B. Kaplan and H. Georgi, *$SU(2) \times U(1)$ Breaking by Vacuum Misalignment*, *Phys. Lett. B* **136** (1984) 183.
- [17] D.B. Kaplan, H. Georgi and S. Dimopoulos, *Composite Higgs Scalars*, *Phys. Lett. B* **136** (1984) 187.
- [18] H. Georgi and D.B. Kaplan, *Composite Higgs and Custodial $SU(2)$* , *Phys. Lett. B* **145** (1984) 216.
- [19] M.J. Dugan, H. Georgi and D.B. Kaplan, *Anatomy of a Composite Higgs Model*, *Nucl. Phys. B* **254** (1985) 299.
- [20] N. Arkani-Hamed, A.G. Cohen and H. Georgi, *Electroweak symmetry breaking from dimensional deconstruction*, *Phys. Lett. B* **513** (2001) 232 [[hep-ph/0105239](#)].

- [21] N. Arkani-Hamed, A.G. Cohen, T. Gregoire and J.G. Wacker, *Phenomenology of electroweak symmetry breaking from theory space*, *JHEP* **08** (2002) 020 [[hep-ph/0202089](#)].
- [22] N. Arkani-Hamed, A.G. Cohen, E. Katz and A.E. Nelson, *The Littlest Higgs*, *JHEP* **07** (2002) 034 [[hep-ph/0206021](#)].
- [23] Z. Chacko, H.-S. Goh and R. Harnik, *The Twin Higgs: Natural electroweak breaking from mirror symmetry*, *Phys. Rev. Lett.* **96** (2006) 231802 [[hep-ph/0506256](#)].
- [24] R. Barbieri, T. Gregoire and L.J. Hall, *Mirror world at the large hadron collider*, [hep-ph/0509242](#).
- [25] Z. Chacko, Y. Nomura, M. Papucci and G. Perez, *Natural little hierarchy from a partially goldstone twin Higgs*, *JHEP* **01** (2006) 126 [[hep-ph/0510273](#)].
- [26] T. de Boer, M. Lindner and A. Trautner, *Electroweak hierarchy from conformal and custodial symmetry*, *Phys. Lett. B* **861** (2025) 139241 [[2407.15920](#)].
- [27] T. Alanne, H. Gertov, F. Sannino and K. Tuominen, *Elementary Goldstone Higgs boson and dark matter*, *Phys. Rev. D* **91** (2015) 095021 [[1411.6132](#)].
- [28] H. Gertov, A. Meroni, E. Molinaro and F. Sannino, *Theory and phenomenology of the elementary Goldstone Higgs boson*, *Phys. Rev. D* **92** (2015) 095003 [[1507.06666](#)].
- [29] A. Davidson, *$B - L$ as the fourth color within an $SU(2)_L \times U(1)_R \times U(1)$ model*, *Phys. Rev. D* **20** (1979) 776.
- [30] R.E. Marshak and R.N. Mohapatra, *Quark - Lepton Symmetry and $B - L$ as the $U(1)$ Generator of the Electroweak Symmetry Group*, *Phys. Lett. B* **91** (1980) 222.
- [31] R.N. Mohapatra and R.E. Marshak, *Local $B - L$ Symmetry of Electroweak Interactions, Majorana Neutrinos and Neutron Oscillations*, *Phys. Rev. Lett.* **44** (1980) 1316.
- [32] C. Wetterich, *Neutrino Masses and the Scale of $B - L$ Violation*, *Nucl. Phys. B* **187** (1981) 343.
- [33] E.E. Jenkins, *Searching for a $(B - L)$ Gauge Boson in $p\bar{p}$ Collisions*, *Phys. Lett. B* **192** (1987) 219.
- [34] W. Buchmuller, C. Greub and P. Minkowski, *Neutrino masses, neutral vector bosons and the scale of $B - L$ breaking*, *Phys. Lett. B* **267** (1991) 395.
- [35] S. Khalil, *Low scale $B - L$ extension of the Standard Model at the LHC*, *J. Phys. G* **35** (2008) 055001 [[hep-ph/0611205](#)].
- [36] P. Sikivie, L. Susskind, M.B. Voloshin and V.I. Zakharov, *Isospin Breaking in Technicolor Models*, *Nucl. Phys. B* **173** (1980) 189.
- [37] M. Sher, *Electroweak Higgs Potentials and Vacuum Stability*, *Phys. Rept.* **179** (1989) 273.
- [38] P. Galison and A. Manohar, *TWO Z 's OR NOT TWO Z 's?*, *Phys. Lett. B* **136** (1984) 279.
- [39] B. Holdom, *Two $U(1)$'s and Epsilon Charge Shifts*, *Phys. Lett. B* **166** (1986) 196.
- [40] J.-X. Pan, M. He, X.-G. He and G. Li, *Scrutinizing a massless dark photon: basis independence*, *Nucl. Phys. B* **953** (2020) 114968 [[1807.11363](#)].
- [41] W. Loinaz and T. Takeuchi, *Charge assignments in multiple $U(1)$ gauge theories*, *Phys. Rev. D* **60** (1999) 115008 [[hep-ph/9903362](#)].

- [42] C.D. Carone and H. Murayama, *Realistic models with a light $U(1)$ gauge boson coupled to baryon number*, *Phys. Rev. D* **52** (1995) 484 [[hep-ph/9501220](#)].
- [43] L.N. Chang, O. Lebedev, W. Loinaz and T. Takeuchi, *Constraints on gauged $B - 3L(\tau)$ and related theories*, *Phys. Rev. D* **63** (2001) 074013 [[hep-ph/0010118](#)].
- [44] A. Aranda and C.D. Carone, *Orthogonal $U(1)$'s, proton stability and extra dimensions*, *Phys. Rev. D* **63** (2001) 075012 [[hep-ph/0012092](#)].
- [45] C.P. Burgess, *Introduction to Effective Field Theory*, *Ann. Rev. Nucl. Part. Sci.* **57** (2007) 329 [[hep-th/0701053](#)].
- [46] A.V. Manohar and E. Nardoni, *Renormalization Group Improvement of the Effective Potential: an EFT Approach*, *JHEP* **04** (2021) 093 [[2010.15806](#)].
- [47] G. 't Hooft, *A Planar Diagram Theory for Strong Interactions*, *Nucl. Phys. B* **72** (1974) 461.
- [48] G. Veneziano, *Some Aspects of a Unified Approach to Gauge, Dual and Gribov Theories*, *Nucl. Phys. B* **117** (1976) 519.
- [49] S.P. Martin, *Two Loop Effective Potential for a General Renormalizable Theory and Softly Broken Supersymmetry*, *Phys. Rev. D* **65** (2002) 116003 [[hep-ph/0111209](#)].
- [50] D. Buttazzo, G. Degrassi, P.P. Giardino, G.F. Giudice, F. Sala, A. Salvio et al., *Investigating the near-criticality of the Higgs boson*, *JHEP* **12** (2013) 089 [[1307.3536](#)].
- [51] L. Sartore and I. Schienbein, *PyR@TE 3*, *Comput. Phys. Commun.* **261** (2021) 107819 [[2007.12700](#)].
- [52] R. Barbieri and G.F. Giudice, *Upper Bounds on Supersymmetric Particle Masses*, *Nucl. Phys. B* **306** (1988) 63.
- [53] G.W. Anderson and D.J. Castano, *Measures of fine tuning*, *Phys. Lett. B* **347** (1995) 300 [[hep-ph/9409419](#)].
- [54] J. Alwall, R. Frederix, S. Frixione, V. Hirschi, F. Maltoni, O. Mattelaer et al., *The automated computation of tree-level and next-to-leading order differential cross sections, and their matching to parton shower simulations*, *JHEP* **07** (2014) 079 [[1405.0301](#)].
- [55] C. Degrande, C. Duhr, B. Fuks, D. Grellscheid, O. Mattelaer and T. Reiter, *UFO - The Universal FeynRules Output*, *Comput. Phys. Commun.* **183** (2012) 1201 [[1108.2040](#)].
- [56] N.D. Christensen and C. Duhr, *FeynRules - Feynman rules made easy*, *Comput. Phys. Commun.* **180** (2009) 1614 [[0806.4194](#)].
- [57] ATLAS collaboration, *Search for high-mass dilepton resonances using 139 fb^{-1} of pp collision data collected at $\sqrt{s} = 13\text{ TeV}$ with the ATLAS detector*, *Phys. Lett. B* **796** (2019) 68 [[1903.06248](#)].
- [58] CMS collaboration, *Search for resonant and nonresonant new phenomena in high-mass dilepton final states at $\sqrt{s} = 13\text{ TeV}$* , *JHEP* **07** (2021) 208 [[2103.02708](#)].
- [59] ATLAS collaboration, *Prospects for searches for heavy Z' and W' bosons in fermionic final states with the ATLAS experiment at the HL-LHC*, .
- [60] T. Konstandin and G. Servant, *Cosmological Consequences of Nearly Conformal Dynamics at the TeV scale*, *JCAP* **12** (2011) 009 [[1104.4791](#)].

- [61] PLANCK collaboration, *Planck 2018 results. VI. Cosmological parameters*, *Astron. Astrophys.* **641** (2020) A6 [1807.06209].
- [62] G. Alguero, G. Belanger, F. Boudjema, S. Chakraborti, A. Goudelis, S. Kraml et al., *micrOMEGAs 6.0: N-component dark matter*, *Comput. Phys. Commun.* **299** (2024) 109133 [2312.14894].
- [63] F. Staub, *SARAH 4 : A tool for (not only SUSY) model builders*, *Comput. Phys. Commun.* **185** (2014) 1773 [1309.7223].
- [64] XENON collaboration, *First Dark Matter Search with Nuclear Recoils from the XENONnT Experiment*, *Phys. Rev. Lett.* **131** (2023) 041003 [2303.14729].
- [65] C.A.J. O’Hare, *New Definition of the Neutrino Floor for Direct Dark Matter Searches*, *Phys. Rev. Lett.* **127** (2021) 251802 [2109.03116].
- [66] DARWIN collaboration, *DARWIN: towards the ultimate dark matter detector*, *JCAP* **11** (2016) 017 [1606.07001].
- [67] A. Alves, S. Profumo and F.S. Queiroz, *The dark Z' portal: direct, indirect and collider searches*, *JHEP* **04** (2014) 063 [1312.5281].
- [68] A. Alves, A. Berlin, S. Profumo and F.S. Queiroz, *Dark Matter Complementarity and the Z' Portal*, *Phys. Rev. D* **92** (2015) 083004 [1501.03490].
- [69] W. Wang and Z.-L. Han, *Radiative linear seesaw model, dark matter, and $U(1)_{B-L}$* , *Phys. Rev. D* **92** (2015) 095001 [1508.00706].
- [70] A. Alves, A. Berlin, S. Profumo and F.S. Queiroz, *Dirac-fermionic dark matter in $U(1)_X$ models*, *JHEP* **10** (2015) 076 [1506.06767].
- [71] T. Jacques, A. Katz, E. Morgante, D. Racco, M. Rameez and A. Riotto, *Complementarity of DM searches in a consistent simplified model: the case of Z'* , *JHEP* **10** (2016) 071 [1605.06513].
- [72] S. Okada, *Z' Portal Dark Matter in the Minimal $B - L$ Model*, *Adv. High Energy Phys.* **2018** (2018) 5340935 [1803.06793].
- [73] ATLAS collaboration, *Constraints on new phenomena via Higgs boson couplings and invisible decays with the ATLAS detector*, *JHEP* **11** (2015) 206 [1509.00672].
- [74] T. Robens and T. Stefaniak, *Status of the Higgs Singlet Extension of the Standard Model after LHC Run 1*, *Eur. Phys. J. C* **75** (2015) 104 [1501.02234].
- [75] A. Falkowski, C. Gross and O. Lebedev, *A second Higgs from the Higgs portal*, *JHEP* **05** (2015) 057 [1502.01361].
- [76] W.D. Goldberger, B. Grinstein and W. Skiba, *Distinguishing the Higgs boson from the dilaton at the Large Hadron Collider*, *Phys. Rev. Lett.* **100** (2008) 111802 [0708.1463].
- [77] Z. Chacko and R.K. Mishra, *Effective Theory of a Light Dilaton*, *Phys. Rev. D* **87** (2013) 115006 [1209.3022].
- [78] B. Bellazzini, C. Csaki, J. Hubisz, J. Serra and J. Terning, *A Higgslike Dilaton*, *Eur. Phys. J. C* **73** (2013) 2333 [1209.3299].
- [79] A. Ahmed, B.M. Dillon, B. Grzadkowski, J.F. Gunion and Y. Jiang, *Implications of the absence of high-mass radion signals*, *Phys. Rev. D* **95** (2017) 095019 [1512.05771].

- [80] A. Ahmed, A. Mariotti and S. Najjari, *A light dilaton at the LHC*, *JHEP* **05** (2020) 093 [1912.06645].
- [81] ILD CONCEPT GROUP collaboration, *International Large Detector: Interim Design Report*, 2003.01116.
- [82] G. Ripellino, M.V. Voorde, A. Gallén and R. Gonzalez Suarez, *Searching for long-lived dark scalars at the FCC-ee*, 2412.10141.
- [83] B. Foster, R. D’Arcy and C.A. Lindstrom, *A hybrid, asymmetric, linear Higgs factory based on plasma-wakefield and radio-frequency acceleration*, *New J. Phys.* **25** (2023) 093037 [2303.10150].
- [84] A. Laudrain, T. Behnke, C.M. Berggren, K. Buesser, F. Gaede, C. Grojean et al., *Physics Performance and Detector Requirements at an Asymmetric Higgs Factory*, *PoS EPS-HEP2023* (2024) 556 [2411.14313].
- [85] PARTICLE DATA GROUP collaboration, *Review of Particle Physics*, *PTEP* **2022** (2022) 083C01.
- [86] R.K. Ellis et al., *Physics Briefing Book: Input for the European Strategy for Particle Physics Update 2020*, 1910.11775.
- [87] A.D. Linde, *Dynamical Symmetry Restoration and Constraints on Masses and Coupling Constants in Gauge Theories*, *JETP Lett.* **23** (1976) 64.
- [88] D. Litim, C. Wetterich and N. Tetradis, *Nonperturbative analysis of the Coleman-Weinberg phase transition*, *Mod. Phys. Lett. A* **12** (1997) 2287 [hep-ph/9407267].
- [89] R. Jinno and M. Takimoto, *Probing a classically conformal B-L model with gravitational waves*, *Phys. Rev. D* **95** (2017) 015020 [1604.05035].
- [90] S. Iso, P.D. Serpico and K. Shimada, *QCD-Electroweak First-Order Phase Transition in a Supercooled Universe*, *Phys. Rev. Lett.* **119** (2017) 141301 [1704.04955].
- [91] C. Marzo, L. Marzola and V. Vaskonen, *Phase transition and vacuum stability in the classically conformal B-L model*, *Eur. Phys. J. C* **79** (2019) 601 [1811.11169].
- [92] J. Ellis, M. Lewicki and V. Vaskonen, *Updated predictions for gravitational waves produced in a strongly supercooled phase transition*, *JCAP* **11** (2020) 020 [2007.15586].
- [93] D. Schmitt and L. Sagunski, *QCD-sourced tachyonic phase transition in a supercooled Universe*, 2409.05851.
- [94] S. Iso, N. Okada and Y. Orikasa, *Resonant Leptogenesis in the Minimal B-L Extended Standard Model at TeV*, *Phys. Rev. D* **83** (2011) 093011 [1011.4769].
- [95] V.V. Khoze and G. Ro, *Leptogenesis and Neutrino Oscillations in the Classically Conformal Standard Model with the Higgs Portal*, *JHEP* **10** (2013) 075 [1307.3764].
- [96] T. Hambye, A. Strumia and D. Teresi, *Super-cool Dark Matter*, *JHEP* **08** (2018) 188 [1805.01473].
- [97] P. Huang and K.-P. Xie, *Leptogenesis triggered by a first-order phase transition*, *JHEP* **09** (2022) 052 [2206.04691].
- [98] A. Dasgupta, P.S.B. Dev, A. Ghoshal and A. Mazumdar, *Gravitational wave pathway to testable leptogenesis*, *Phys. Rev. D* **106** (2022) 075027 [2206.07032].

- [99] A. Das and Y. Orikasa, *Resonant leptogenesis in minimal $U(1)_X$ extensions of the Standard Model*, 2407.05644.
- [100] G. Chauhan, *Collider Tests of Flavored Resonant Leptogenesis in the $U(1)_X$ Model*, 2407.09460.
- [101] J. Braun and H. Gies, *Chiral phase boundary of QCD at finite temperature*, *JHEP* **06** (2006) 024 [[hep-ph/0602226](#)].
- [102] F. Cuteri, O. Philipsen and A. Sciarra, *On the order of the QCD chiral phase transition for different numbers of quark flavours*, *JHEP* **11** (2021) 141 [[2107.12739](#)].
- [103] L. Marzola, A. Racioppi and V. Vaskonen, *Phase transition and gravitational wave phenomenology of scalar conformal extensions of the Standard Model*, *Eur. Phys. J. C* **77** (2017) 484 [[1704.01034](#)].
- [104] T. Prokopec, J. Rezaeck and B. Świeżewska, *Gravitational waves from conformal symmetry breaking*, *JCAP* **02** (2019) 009 [[1809.11129](#)].
- [105] L. Sagunski, P. Schicho and D. Schmitt, *Supercool exit: Gravitational waves from QCD-triggered conformal symmetry breaking*, *Phys. Rev. D* **107** (2023) 123512 [[2303.02450](#)].
- [106] S. Kawai and N. Okada, *Reheating consistency condition on the classically conformal $U(1)_{B-L}$ Higgs inflation model*, *Phys. Rev. D* **108** (2023) 015013 [[2303.00342](#)].
- [107] C.D. Froggatt and H.B. Nielsen, *Standard model criticality prediction: Top mass 173 ± 5 -GeV and Higgs mass 135 ± 9 -GeV*, *Phys. Lett. B* **368** (1996) 96 [[hep-ph/9511371](#)].
- [108] D.F. Litim and F. Sannino, *Asymptotic safety guaranteed*, *JHEP* **12** (2014) 178 [[1406.2337](#)].
- [109] J.C. Pati and A. Salam, *Lepton Number as the Fourth Color*, *Phys. Rev. D* **10** (1974) 275.
- [110] J.C. Montero and V. Pleitez, *Gauging $U(1)$ symmetries and the number of right-handed neutrinos*, *Phys. Lett. B* **675** (2009) 64 [[0706.0473](#)].
- [111] E. Ma and R. Srivastava, *Dirac or inverse seesaw neutrino masses with $B - L$ gauge symmetry and S_3 flavor symmetry*, *Phys. Lett. B* **741** (2015) 217 [[1411.5042](#)].
- [112] E. Ma, N. Pollard, R. Srivastava and M. Zakeri, *Gauge $B - L$ Model with Residual Z_3 Symmetry*, *Phys. Lett. B* **750** (2015) 135 [[1507.03943](#)].
- [113] C. Bonilla, S. Centelles-Chuliá, R. Cepedello, E. Peinado and R. Srivastava, *Dark matter stability and Dirac neutrinos using only Standard Model symmetries*, *Phys. Rev. D* **101** (2020) 033011 [[1812.01599](#)].
- [114] X.G. He, G.C. Joshi, H. Lew and R.R. Volkas, *NEW Z-prime PHENOMENOLOGY*, *Phys. Rev. D* **43** (1991) 22.
- [115] S. Baek, N.G. Deshpande, X.G. He and P. Ko, *Muon anomalous $g-2$ and gauged $L(\mu) - L(\tau)$ models*, *Phys. Rev. D* **64** (2001) 055006 [[hep-ph/0104141](#)].
- [116] E. Ma, D.P. Roy and S. Roy, *Gauged $L(\mu) - L(\tau)$ with large muon anomalous magnetic moment and the bimaximal mixing of neutrinos*, *Phys. Lett. B* **525** (2002) 101 [[hep-ph/0110146](#)].
- [117] J. Heck and W. Rodejohann, *Gauged $L_\mu - L_\tau$ Symmetry at the Electroweak Scale*, *Phys. Rev. D* **84** (2011) 075007 [[1107.5238](#)].

- [118] W. Altmannshofer, S. Gori, M. Pospelov and I. Yavin, *Neutrino Trident Production: A Powerful Probe of New Physics with Neutrino Beams*, *Phys. Rev. Lett.* **113** (2014) 091801 [1406.2332].
- [119] W. Altmannshofer, M. Carena and A. Crivellin, *$L_\mu - L_\tau$ theory of Higgs flavor violation and $(g - 2)_\mu$* , *Phys. Rev. D* **94** (2016) 095026 [1604.08221].
- [120] J. Kubo, J. Kuntz, M. Lindner, J. Rezaeck, P. Saake and A. Trautner, *Unified emergence of energy scales and cosmic inflation*, *JHEP* **08** (2021) 016 [2012.09706].
- [121] J. Kubo, M. Lindner, K. Schmitz and M. Yamada, *Planck mass and inflation as consequences of dynamically broken scale invariance*, *Phys. Rev. D* **100** (2019) 015037 [1811.05950].
- [122] N. Okada and Q. Shafi, *Observable Gravity Waves From $U(1)_{B-L}$ Higgs and Coleman-Weinberg Inflation*, 1311.0921.
- [123] S. Oda, N. Okada, D. Raut and D.-s. Takahashi, *Nonminimal quartic inflation in classically conformal $U(1)_X$ extended standard model*, *Phys. Rev. D* **97** (2018) 055001 [1711.09850].